Published for SISSA by Springer

Received: November 23, 2018
Revised: January 23, 2019
Accepted: February 16, 2019
Published: February 22, 2019

Vacuum structure of the left-right symmetric model

P.S. Bhupal Dev,[a] **Rabindra N. Mohapatra,**[b] **Werner Rodejohann**[c] **and Xun-Jie Xu**[c]

[a] *Department of Physics and McDonnell Center for the Space Sciences, Washington University, St. Louis, MO 63130, U.S.A.*

[b] *Maryland Center for Fundamental Physics and Department of Physics, University of Maryland, College Park, MD 20742, U.S.A.*

[c] *Max-Planck-Institut für Kernphysik, Postfach 103980, Heidelberg D-69029, Germany*

E-mail: bdev@wustl.edu, rmohapat@physics.umd.edu, werner.rodejohann@mpi-hd.mpg.de, xunjie@mpi-hd.mpg.de

Abstract: The left-right symmetric model (LRSM), originally proposed to explain parity violation in low energy processes, has since emerged as an attractive framework for light neutrino masses via the seesaw mechanism. The scalar sector of the minimal LRSM consists of an SU(2) bi-doublet, as well as left- and right-handed weak isospin triplets, thus making the corresponding vacuum structure much more complicated than that of the Standard Model. In particular, the desired ground state of the Higgs potential should be a charge conserving, and preferably global, minimum with parity violation at low scales. We show that this is not a generic feature of the LRSM potential and happens only for a small fraction of the parameter space of the potential. We also analytically study the potential for some simplified cases and obtain sufficient conditions (though not necessary) to achieve successful symmetry breaking. We then carry out a detailed statistical analysis of the minima of the Higgs potential using numerical minimization and find that for a large fraction of the parameter space, the potential does not have a good vacuum. Imposing the analytically obtained conditions, we can readily find the small part of the parameter space with good vacua. Consequences for some scalar masses are also discussed.

Keywords: Beyond Standard Model, Spontaneous Symmetry Breaking, Higgs Physics, Neutrino Physics

ArXiv ePrint: 1811.06869

https://doi.org/10.1007/JHEP02(2019)154

JHEP02(2019)154

Contents

JHEP02(2019)154

1 Introduction

The discovery of neutrino masses is a sure sign of new physics beyond the Standard Model (SM). A simple paradigm for neutrino masses is the seesaw mechanism [1–5] which introduces right-handed neutrinos (RHN) with heavy Majorana masses. Two questions then arise: (i) what is the seesaw scale or the mass of the RHNs? and (ii) what is the ultraviolet (UV)-complete theory that leads naturally to the basic ingredients inherent in the seesaw mechanism i.e. RHNs and a $B-L$ symmetry whose breaking gives rise to their Majorana masses? Two classes of theories with this property are: (i) the SO(10) model whose basic spinor representation contains the RHN and which contains a group generator that is the $B-L$ local symmetry [6], and (ii) the left-right symmetric model (LRSM) [7–9], which is the simplest extension of the SM that contains three RHNs to cancel the gauge anomalies and $B-L$ symmetry as a natural symmetry [10].

In this paper, we focus on symmetry breaking aspects of the minimal LRSM and carry out an analysis of its vacuum structure. The general procedure to investigate this is to write down the Higgs potential involving the various scalar multiplets of the LR gauge group $\mathrm{SU}(2)_L \otimes \mathrm{SU}(2)_R \otimes \mathrm{U}(1)_{B-L}$ and look for the minimum of the potential that breaks the gauge symmetry down to $\mathrm{U}(1)_{\mathrm{em}}$. Morever, the theory should be parity violating at low scale and generate naturally small neutrino masses. The detailed analysis of the non-supersymmetric LRSM Higgs potential and its minima have been discussed in many works [11–27] (supersymmetric LRSM Higgs sectors have been studied in refs. [28, 29]).

It is known that for certain ranges of the parameters (e.g. negative scalar mass squares and positive values for scalar couplings), a desired (good) vacuum is obtained. However, if all the couplings are chosen randomly to start with, it is not clear how often one gets a good vacuum. Secondly, it is not known whether those minima obtained above are global minima of the potential or are simply the local ones. Third, the boundedness-from-below of the potential has been used as the necessary and sufficient condition for vacuum stability [18, 19], but as we show in this paper, a bounded-from-below potential is necessary for a good vacuum, but not sufficient.

We use the gauge freedom of the theory to give simple criteria that are to be fulfilled in order to end up in a good vacuum (i.e. charge conserving and parity violating at low scales). Keeping arbitrary values for the parameters of the Higgs potential we furthermore check for what fraction of the parameter space a global minimum with desired properties is obtained. Once a range of the parameters is determined where a global minimum occurs, one can then use them to find the scalar spectrum corresponding to that choice, which is a potential test of the model. We do not carry out an exhaustive analysis of the scalar masses but rather give some simple examples at viable minima of the model.

The paper is organized as follows. In section 2, we review the details of the model and its scalar sector. In section 3, we write down the full scalar potential and give criteria for obtaining the good vacua of the model. In section 4 we present analytical studies focused on some simplified cases, followed by numerical studies to scan the whole parameter space in section 5. Finally we summarize and conclude in section 6. Some technical details are delegated to the appendix.

2 Model details

The LRSM [7–9] extends the SM gauge group $\mathcal{G}_{\rm SM} \equiv {\rm SU}(3)_c \otimes {\rm SU}(2)_L \otimes {\rm U}(1)_Y$ to $\mathcal{G}_{\rm LR} \equiv {\rm SU}(3)_c \otimes {\rm SU}(2)_L \otimes {\rm SU}(2)_R \otimes {\rm U}(1)_{B-L}$. The quarks and leptons are assigned to the following irreducible representations of $\mathcal{G}_{\rm LR}$:

$$Q_{L,i} = \begin{pmatrix} u_L \\ d_L \end{pmatrix}_i : \left(\mathbf{3}, \mathbf{2}, \mathbf{1}, \frac{1}{3}\right), \qquad Q_{R,i} = \begin{pmatrix} u_R \\ d_R \end{pmatrix}_i : \left(\mathbf{3}, \mathbf{1}, \mathbf{2}, \frac{1}{3}\right), \tag{2.1}$$

$$\psi_{L,i} = \begin{pmatrix} \nu_L \\ e_L \end{pmatrix}_i : (\mathbf{1}, \mathbf{2}, \mathbf{1}, -1), \qquad \psi_{R,i} = \begin{pmatrix} N_R \\ e_R \end{pmatrix}_i : (\mathbf{1}, \mathbf{1}, \mathbf{2}, -1), \tag{2.2}$$

where $i = 1, 2, 3$ represents the family index, and the subscripts L, R denote the left- and right-handed chiral projection operators $P_{L,R} = (1 \mp \gamma_5)/2$, respectively. The B and L charges are fixed using the electric charge formula [10]

$$Q = I_{3L} + I_{3R} + \frac{B - L}{2}. \tag{2.3}$$

In the scalar sector, a bi-doublet (ϕ) and two triplets (Δ_L, Δ_R) are introduced with the following quantum number assignments under $\mathcal{G}_{\rm LR}$:

$$\phi : (\mathbf{1}, \mathbf{2}, \mathbf{2}, 0), \qquad \Delta_L : (\mathbf{1}, \mathbf{3}, \mathbf{1}, 2), \qquad \Delta_R : (\mathbf{1}, \mathbf{1}, \mathbf{3}, 2). \tag{2.4}$$

JHEP02(2019)154

It is conventional to adopt the matrix representation in which ϕ and $\Delta_{L,R}$ are written as

$$\phi = \begin{pmatrix} \phi_1^0 & \phi_1^+ \\ \phi_2^- & \phi_2^0 \end{pmatrix}, \qquad \Delta_L = \begin{pmatrix} \delta_L^+/\sqrt{2} & \delta_L^{++} \\ \delta_L^0 & -\delta_L^+/\sqrt{2} \end{pmatrix}, \qquad \Delta_R = \begin{pmatrix} \delta_R^+/\sqrt{2} & \delta_R^{++} \\ \delta_R^0 & -\delta_R^+/\sqrt{2} \end{pmatrix}. \tag{2.5}$$

The corresponding transformation rules are

$$\mathrm{SU}(2)_L \otimes \mathrm{SU}(2)_R: \quad \phi \to U_L \phi U_R^\dagger, \quad \Delta_L \to U_L \Delta_L U_L^\dagger, \quad \Delta_R \to U_R \Delta_R U_R^\dagger, \tag{2.6}$$

$$\mathrm{U}(1)_{B-L}: \quad \phi \to \phi, \quad \Delta_L \to e^{i\theta_{B-L}} \Delta_L, \quad \Delta_R \to e^{i\theta_{B-L}} \Delta_R, \tag{2.7}$$

for $U_L \in \mathrm{SU}(2)_L$, $U_R \in \mathrm{SU}(2)_R$ and $e^{i\theta_{B-L}} \in \mathrm{U}(1)_{B-L}$. Note that $\tilde{\phi} \equiv \sigma_2 \phi^* \sigma_2 = -\epsilon \phi^* \epsilon$ transforms in the same way as ϕ.

The model also has a discrete left-right symmetry, which can either be the $\mathcal{P}$ parity or the $\mathcal{C}$ parity:

$$\mathcal{P}: \quad \phi \to \phi^\dagger, \quad \Delta_L \leftrightarrow \Delta_R, \tag{2.8}$$

$$\mathcal{C}: \quad \phi \to \phi^T, \quad \Delta_L \leftrightarrow \Delta_R^*. \tag{2.9}$$

The scalar potential with $\mathcal{P}$ parity is more constrained than that with $\mathcal{C}$ parity[1] as the latter allows several complex phases. In this paper, for simplicity, we assume all the couplings in the scalar potential to be real, i.e. there is no explicit CP violation[2] in the potential. Such a potential respects both parities.

In general the full potential contains 17 gauge invariant renormalisable terms [14]. After spontaneous symmetry breaking, some components of ϕ and $\Delta_{L,R}$ obtain nonzero vacuum expectation values (VEVs) while the others do not, depending on the parameters of the potential. Since the gauge symmetry $\mathrm{SU}(2)_L \otimes \mathrm{SU}(2)_R \otimes \mathrm{U}(1)_{B-L}$ is required to break to $\mathrm{U}(1)_{\mathrm{em}}$ by these scalar fields, the desired VEV alignment is [14]

$$\langle \phi \rangle = \frac{1}{\sqrt{2}} \begin{pmatrix} \kappa_1 & 0 \\ 0 & \kappa_2 e^{i\theta_2} \end{pmatrix}, \qquad \langle \Delta_L \rangle = \frac{1}{\sqrt{2}} \begin{pmatrix} 0 & 0 \\ v_L e^{i\theta_L} & 0 \end{pmatrix}, \qquad \langle \Delta_R \rangle = \frac{1}{\sqrt{2}} \begin{pmatrix} 0 & 0 \\ v_R & 0 \end{pmatrix}. \tag{2.10}$$

The VEVs should furthermore obey the hierarchy $v_L \ll \kappa_{1,2} \ll v_R$ (v_L may vanish) to meet the known phenomenology, such as tiny neutrino masses, heavy RH gauge boson masses, the electroweak precision parameter $\rho \simeq 1$, etc.

Although eq. (2.10) is what we need to successfully achieve spontaneous symmetry breaking in the LRSM, for general (arbitrary) values of the parameters, the scalar potential does not necessarily lead to this VEV alignment. For example, if we minimize the scalar potential we may obtain a minimum with nonzero diagonal VEVs of $\langle \Delta_L \rangle$ or $\langle \Delta_R \rangle$, which would break $\mathrm{U}(1)_{\mathrm{em}}$. It is also possible to get a minimum with $\langle \Delta_L \rangle = \langle \Delta_R \rangle$ which would imply unbroken parity symmetry. The various possibilities of symmetry breaking with the full scalar potential of LRSM, due to the considerable complexity, have never been comprehensively studied before.

[1] See eqs. (9) and (10) in ref. [25] for comparison.

[2] We do, however, find that a small portion of the randomly generated samples in section 5 have complex VEVs though the potential parameters are real, which implies that spontaneous CP violation is possible in this model. See refs. [11–14, 16, 17] for more details.

JHEP02(2019)154

In this paper, we will therefore address an essential question of the spontaneous symmetry breaking in the LRSM:

How can we obtain the VEV alignment in eq. (2.10) and how likely is this?

Since the full scalar potential is very complicated, a purely analytical study is difficult and we mainly adopt a numerical approach. However, we provide some illustrative analytical studies for simplified cases, where a lot of terms in the potential are absent. Nevertheless, the analytical results give us some useful insight into the vacuum structure of the scalar potential and serve as a supplement to the full numerical calculations. Our numerical approach has already been established in refs. [30–32] to successfully analyze beyond the SM scalar potentials. In general, given specific values of the potential parameters, we can always use a computer program to numerically minimize the potential and obtain a minimum. With further developed algorithms (see the details presented in section 5), we can make the program capable of identifying the zero entries in eq. (2.10). In this way we can find out all possible VEV alignments that can be obtained in the LRSM potential. We choose not to use the `Vevacious` package [35], which, among other things, can also provide the minima of beyond the SM scalar potentials. This package currently has limited capability to the case we are interested in, since our potential contains many parameters and field components that can obtain a VEV. In addition, we will perform a statistical analysis with a large number of random samples. Hence, we use a self-written dedicated minimization program, which we have made publicly available in `GitHub` [36].

As noted earlier, the significance of such a study is two-fold. First of all, for any given set of potential parameters, we can infer whether it can lead to successful symmetry breaking and whether the minimum of the potential is a global minimum. This in turn can put constraints on the potential parameters and also on the scalar mass spectrum. If the LRSM is taken as a serious theory of particle interactions beyond the SM, then these theoretical constraints from vacuum stability should be taken into consideration, in combination with other theoretical constraints, such as unitarity and perturbativity [23, 24, 37], as well as experimental constraints from lepton flavor violation, neutrinoless double beta decay, rare meson decays and colliders [38–56].

Secondly, for extended LRSMs with modified scalar sectors, e.g. with additional scalar bi-doublets, triplets, singlets, etc. [57–69], one would again be concerned about the question of whether the desired VEVs can be obtained. While the potential for such cases may be too complicated to repeat the analytical calculations given here, our numerical method can be easily implemented to analyze the vacuum structures of such models. We leave these studies for future work.

3 The scalar potential

The most general gauge invariant scalar potential invariant under eq. (2.6) contains 17 independent terms:

$$\begin{aligned} V \;=\; & -\mu_1^2 \mathrm{Tr}[\phi^\dagger\phi] - \mu_2^2 \left(\mathrm{Tr}[\tilde{\phi}\phi^\dagger] + \mathrm{Tr}[\tilde{\phi}^\dagger\phi]\right) - \mu_3^2 \left(\mathrm{Tr}[\Delta_L\Delta_L^\dagger] + \mathrm{Tr}[\Delta_R\Delta_R^\dagger]\right) + \lambda_1 \left(\mathrm{Tr}[\phi^\dagger\phi]\right)^2 \\ & + \lambda_2 \left(\left(\mathrm{Tr}[\tilde{\phi}\phi^\dagger]\right)^2 + \left(\mathrm{Tr}[\tilde{\phi}^\dagger\phi]\right)^2\right) + \lambda_3 \mathrm{Tr}[\tilde{\phi}\phi^\dagger]\mathrm{Tr}[\tilde{\phi}^\dagger\phi] + \lambda_4 \mathrm{Tr}[\phi^\dagger\phi]\left(\mathrm{Tr}[\tilde{\phi}\phi^\dagger] + \mathrm{Tr}[\tilde{\phi}^\dagger\phi]\right) \end{aligned}$$

JHEP02(2019)154

$$
\begin{aligned}
&+\rho_1\left(\left(\mathrm{Tr}[\Delta_L\Delta_L^\dagger]\right)^2+\left(\mathrm{Tr}[\Delta_R\Delta_R^\dagger]\right)^2\right)+\rho_2\left(\mathrm{Tr}[\Delta_L\Delta_L]\mathrm{Tr}[\Delta_L^\dagger\Delta_L^\dagger]+\mathrm{Tr}[\Delta_R\Delta_R]\mathrm{Tr}[\Delta_R^\dagger\Delta_R^\dagger]\right)\\
&+\rho_3\mathrm{Tr}[\Delta_L\Delta_L^\dagger]\mathrm{Tr}[\Delta_R\Delta_R^\dagger]+\rho_4\left(\mathrm{Tr}[\Delta_L\Delta_L]\mathrm{Tr}[\Delta_R^\dagger\Delta_R^\dagger]+\mathrm{Tr}[\Delta_L^\dagger\Delta_L^\dagger]\mathrm{Tr}[\Delta_R\Delta_R]\right)\\
&+\alpha_1\mathrm{Tr}[\phi^\dagger\phi]\left(\mathrm{Tr}[\Delta_L\Delta_L^\dagger]+\mathrm{Tr}[\Delta_R\Delta_R^\dagger]\right)+\alpha_3\left(\mathrm{Tr}[\phi\phi^\dagger\Delta_L\Delta_L^\dagger]+\mathrm{Tr}[\phi^\dagger\phi\Delta_R\Delta_R^\dagger]\right)\\
&+\alpha_2\left(\mathrm{Tr}[\Delta_L\Delta_L^\dagger]\mathrm{Tr}[\tilde{\phi}\phi^\dagger]+\mathrm{Tr}[\Delta_R\Delta_R^\dagger]\mathrm{Tr}[\tilde{\phi}^\dagger\phi]+\mathrm{H.c.}\right)\\
&+\beta_1\left(\mathrm{Tr}[\phi\Delta_R\phi^\dagger\Delta_L^\dagger]+\mathrm{Tr}[\phi^\dagger\Delta_L\phi\Delta_R^\dagger]\right)+\beta_2\left(\mathrm{Tr}[\tilde{\phi}\Delta_R\phi^\dagger\Delta_L^\dagger]+\mathrm{Tr}[\tilde{\phi}^\dagger\Delta_L\phi\Delta_R^\dagger]\right)\\
&+\beta_3\left(\mathrm{Tr}[\phi\Delta_R\tilde{\phi}^\dagger\Delta_L^\dagger]+\mathrm{Tr}[\phi^\dagger\Delta_L\tilde{\phi}\Delta_R^\dagger]\right),
\end{aligned}
\tag{3.1}
$$

where, as we mentioned above, all couplings are assumed real. The spontaneous symmetry breaking in such a complicated potential may result in various types of VEV alignments. Some of them may successfully achieve the desired symmetry breaking given by eq. (2.10) and have phenomenologically viable consequences whereas some may not. In what follows, for convenience, we will refer to the former as *good vacua* and the later as *bad vacua*.

3.1 Good vacua

Since the electromagnetic gauge symmetry $\mathrm{U}(1)_{\mathrm{em}}$ should not be broken in any extension of the SM, only the electric neutral components (namely ϕ_1^0, ϕ_2^0, δ_L^0 and δ_R^0) can acquire nonzero VEVs. In general, the charge conserving VEVs of ϕ, Δ_L and Δ_R should be

$$
\langle\phi\rangle=\frac{1}{\sqrt{2}}\begin{pmatrix}\kappa_1 e^{i\theta_1} & 0\\ 0 & \kappa_2 e^{i\theta_2}\end{pmatrix},\qquad \langle\Delta_L\rangle=\frac{1}{\sqrt{2}}\begin{pmatrix}0 & 0\\ v_L e^{i\theta_L} & 0\end{pmatrix},\qquad \langle\Delta_R\rangle=\frac{1}{\sqrt{2}}\begin{pmatrix}0 & 0\\ v_R e^{i\theta_R} & 0\end{pmatrix}.
\tag{3.2}
$$

However, two of the phases (let us take θ_1 and θ_R) can be removed by the transformation (2.6) with

$$
U_L=\begin{pmatrix}e^{-i\left(\theta_1-\frac{1}{2}\theta_R\right)} & 0\\ 0 & e^{i\left(\theta_1-\frac{1}{2}\theta_R\right)}\end{pmatrix},\qquad U_R=\begin{pmatrix}e^{i\theta_R/2} & 0\\ 0 & e^{-i\theta_R/2}\end{pmatrix}.
\tag{3.3}
$$

Meanwhile, θ_2 and θ_L are transformed to $\theta_2+\theta_1$ and $\theta_L+2\theta_1-\theta_R$, which for simplicity can be redefined as θ_2 and θ_L. Therefore, without loss of generality, one can always set

$$
\theta_1=\theta_R=0\,,
\tag{3.4}
$$

which reduces eq. (3.2) to eq. (2.10). Assuming the potential has a minimum for the VEVs given by eq. (2.10), one can replace the fields with their VEVs and derive the minimization conditions:

$$
\frac{\partial V}{\partial\kappa_1}=\frac{\partial V}{\partial\kappa_2}=\frac{\partial V}{\partial v_L}=\frac{\partial V}{\partial v_R}=\frac{\partial V}{\partial\theta_2}=\frac{\partial V}{\partial\theta_L}=0\,.
\tag{3.5}
$$

From eq. (3.5) one can derive (see appendix A) the renowned seesaw relation of VEVs in LRSM [70]:

$$
\beta_1\kappa_1\kappa_2\cos\left(\theta_2-\theta_L\right)+\beta_2\kappa_1^2\cos\theta_L+\beta_3\kappa_2^2\cos\left(2\theta_2-\theta_L\right)=(2\rho_1-\rho_3)v_Lv_R.
\tag{3.6}
$$

The left-hand side is roughly of the order βv^2 where $\beta=\beta_{1,2,3}$ and $v=246\,\mathrm{GeV}$, and the right-hand side is $\rho\,v_Lv_R$ where $\rho\equiv2\rho_1-\rho_3$. From $\beta v^2=\rho\,v_Lv_R$, one can see that for very

JHEP02(2019)154

large v_R (correspondingly very heavy W_R), v_L will be suppressed by $1/v_R$, corresponding to very tiny neutrino masses, known as the seesaw relation of the VEVs.

Here we would like to give two comments.

- Eq. (3.6) holds only if $v_L^2 \neq v_R^2$. If $v_L^2 = v_R^2$, then the VEVs (κ_1, κ_2, v_L, and v_R) may violate the relation (3.6) while the derivatives in eq. (3.5) remain zero. This can be seen from the analytical calculations in appendix A and is also verified in our numerical studies. Despite that $v_L^2 = v_R^2$ is phenomenologically not allowed (since parity is not broken in this case), it turns out that this case appears much more frequently in the numerical scan than the case with $v_L^2 \neq v_R^2$. Therefore, if in numerical studies a minimum is obtained with the same VEV alignments as in eq. (3.2), one should carefully check whether $v_L^2 = v_R^2$. Only when $v_L^2 \neq v_R^2$, it is a good vacuum with the VEVs satisfiying the seesaw relation (3.6).

- Eq. (3.5) is based on the assumption that a minimum in the form of eq. (3.2) exists. The six equations in (3.5) can (in general) always be solved with respect to the six variables (κ_1, κ_2, v_L, v_R, θ_2, θ_L). However, the existence of solutions of eq. (3.5) implies neither the existence of the minimum, nor that the first-order derivatives with respect to the fields vanish, i.e. $\partial V/\partial\varphi = 0$, where φ stands for all components of ϕ and $\Delta_{L,R}$.

3.2 Bad vacua

Next, we shall investigate other vacua that could appear but would lead to unacceptable physical or phenomenological consequences, e.g. $\mathrm{U}(1)_{\mathrm{em}}$ breaking. Without the requirement of charge conservation, in general, any components of ϕ and $\Delta_{L,R}$ could acquire nonzero VEVs. But before we put nonzero VEVs arbitrarily, we need to examine the symmetries in the potential to avoid considering redundant cases.

First of all, there is the gauge symmetry $\mathrm{SU}(2)_L \otimes \mathrm{SU}(2)_R \otimes \mathrm{U}(1)_{B-L}$, which allows one to remove some degrees of freedom (DOF) in the scalar fields by gauge fixing. By analogy to the SM case, where the Higgs doublet in the unitarity gauge has only one DOF (the physical Higgs boson), in the LRSM we can adopt a similar gauge to remove $3+3+1=7$ DOFs, equal to the number of gauge bosons. More specifically, we use the transformations U_L and U_R in eq. (2.6) to diagonalize ϕ (not $\langle\phi\rangle$) so that

$$\phi = \begin{pmatrix} \phi_1 e^{i\theta_1} & 0 \\ 0 & \phi_2 e^{i\theta_2} \end{pmatrix}, \qquad \Delta_L = \begin{pmatrix} \frac{b_1}{\sqrt{2}} e^{i\omega_2} & c_1 e^{i\omega_3} \\ a_1 e^{i\omega_1} & -\frac{b_1}{\sqrt{2}} e^{i\omega_2} \end{pmatrix}, \qquad \Delta_R = \begin{pmatrix} \frac{b_2}{\sqrt{2}} e^{i\omega_2'} & c_2 e^{i\omega_3'} \\ a_2 e^{i\omega_1'} & -\frac{b_2}{\sqrt{2}} e^{i\omega_2'} \end{pmatrix}. \tag{3.7}$$

Some phases can be further removed by eq. (3.3) and $\mathrm{U}(1)_{B-L}$ transformations[3] so that one can further set

$$\theta_1 = \omega_1' = \omega_2' = 0\,. \tag{3.8}$$

As one can check, indeed seven DOFs have been removed.

[3]The explicit phase removing process to get eq. (3.8) is as follows. First, $\mathrm{U}(1)_{B-L}$ allows overall phase transformations of Δ_L and Δ_R, which can be used to make the diagonal part of Δ_R real, i.e. $\omega_2' = 0$. Then one applies eq. (3.3) to remove phases in the 1–1 and 2–1 entries of ϕ and Δ_R respectively. The phases of the diagonal parts of Δ_L and Δ_R will not be changed by eq. (3.3).

JHEP02(2019)154

Secondly, a vacuum with $\langle\phi_1\rangle = \langle\phi_2\rangle$ and nonzero $\langle b_{1,2}\rangle$ or $\langle c_{1,2}\rangle$ does not necessarily break $\mathrm{U}(1)_{\mathrm{em}}$ due to additional symmetries in the vacuum. Note that if $\langle\phi_1\rangle = \langle\phi_2\rangle$, then $\langle\phi\rangle$ is invariant under

$$\langle\phi\rangle \to U_L\langle\phi\rangle U_R^\dagger, \qquad U_R = U_L \begin{pmatrix} 1 & 0 \\ 0 & e^{i\theta_2} \end{pmatrix}, \tag{3.9}$$

where U_L can be any SU(2) matrix. Accordingly, $\langle\Delta_L\rangle$ and $\langle\Delta_R\rangle$ will be transformed by the above U_L and U_R to other forms. For example, if $\theta_2 = 0$ and the following identical textures of $\langle\Delta_{L,R}\rangle$ are realized,

$$\langle\Delta_L\rangle \propto \langle\Delta_R\rangle \propto \begin{pmatrix} 1 & -1 \\ 1 & -1 \end{pmatrix}, \tag{3.10}$$

then one could choose the following $U_{L,R}$ transformations:

$$U_L = U_R = \frac{1}{\sqrt{2}} \begin{pmatrix} 1 & -1 \\ 1 & 1 \end{pmatrix}. \tag{3.11}$$

It is now straightforward to show that one obtains the same VEV alignment as in eq. (2.10). This implies that the vacuum in this example is physically equivalent to the charge-conserving vacuum.

Considering a general $\mathrm{SU}(2) \otimes \mathrm{U}(1)$ symmetry broken by a triplet (denoted as Δ), we would like to discuss the possible remnant symmetries. If only the 2–1 matrix entry of Δ acquires a VEV, we already know that there is a remnant U(1) symmetry. If only the 1–2 entry acquires a VEV, in a similar way one can also find a remnant U(1). For other VEV alignments, it becomes more complicated. Sometimes even if all the components acquire nonzero VEVs, there is still a remnant U(1), as we have just shown in the above example. To determine the remnant symmetry for general VEVs, one can straightforwardly solve the equation

$$U\langle\Delta\rangle U^\dagger = e^{i\theta}\langle\Delta\rangle \tag{3.12}$$

with respect to $U \in \mathrm{SU}(2)$ and $e^{i\theta} \in \mathrm{U}(1)$. For example, one can find that if the 2–1, 1–1, and 2–2 entries acquire VEVs, then $\mathrm{SU}(2)\otimes\mathrm{U}(1)$ will be completely broken. If only the 1–1 and 2–2 entries acquire VEVs, then SU(2) will be broken to SO(2) and the original U(1) is completely broken. If all the entries acquire nonzero VEVs, in general, $\mathrm{SU}(2) \otimes \mathrm{U}(1)$ is completely broken, unless the determinant of $\langle\Delta\rangle$ is zero. All these conclusions can be derived by solving eq. (3.12).

A necessary and sufficient condition to infer whether $\langle\Delta_L\rangle$ and $\langle\Delta_R\rangle$ really break $\mathrm{U}(1)_{\mathrm{em}}$ in the absence of $\langle\phi\rangle$ is that $\mathrm{U}(1)_{\mathrm{em}}$ is not broken *if and only if*

$$\det\langle\Delta_L\rangle = \det\langle\Delta_R\rangle = 0\,. \tag{3.13}$$

It is straightforward to see that if $\mathrm{U}(1)_{\mathrm{em}}$ is not broken, then the determinants must be zero. The converse, however, needs a short proof: first, note that in the absence of $\langle\phi\rangle$, for

JHEP02(2019)154

any $\langle\Delta_L\rangle$ and $\langle\Delta_R\rangle$, we can always transform them via the Schur decomposition[4] to the following form:

$$\langle\Delta_L\rangle \to U_L\langle\Delta_L\rangle U_L^\dagger = \frac{1}{\sqrt{2}}\begin{pmatrix} x_L & 0 \\ v_L & -x_L \end{pmatrix}, \qquad \langle\Delta_R\rangle \to U_R\langle\Delta_R\rangle U_R^\dagger = \frac{1}{\sqrt{2}}\begin{pmatrix} x_R & 0 \\ v_R & -x_R \end{pmatrix}. \tag{3.14}$$

The determinants $\det\langle\Delta_L\rangle = x_L^2$ and $\det\langle\Delta_R\rangle = x_R^2$ imply that if they are zero, the diagonal elements in eq. (3.14) must be zero, hence $\mathrm{U}(1)_{\mathrm{em}}$ is conserved if one makes arbitrary $\mathrm{SU}(2)_L \otimes \mathrm{SU}(2)_R$ transformations.

However, in the presence of $\langle\phi\rangle$ such transformations may be partially or fully forbidden, depending on whether $\langle\phi_1\rangle = \langle\phi_2\rangle$ or not. In this case, it could be that $\langle\Delta_L\rangle$ and $\langle\Delta_R\rangle$ with zero determinants break $\mathrm{U}(1)_{\mathrm{em}}$. But in our numerical study presented in section 5, among a large number of randomly generated samples, we do not find any samples belonging to this exotic category. Therefore, based on a high-statistics numerical study, we can draw the conclusion that in the presence of $\langle\phi\rangle$, generally $\det\langle\Delta_L\rangle = \det\langle\Delta_R\rangle = 0$ is sufficient to ensure the conservation of $\mathrm{U}(1)_{\mathrm{em}}$.

Finally, some discrete symmetries may connect the vacuum in eq. (2.10) to other vacua. Consider the following two vacua:

$$\text{Vac. 1:}\quad \langle\phi\rangle = \frac{1}{\sqrt{2}}\begin{pmatrix} \kappa_2 e^{i\theta_2} & 0 \\ 0 & \kappa_1 \end{pmatrix}, \quad \langle\Delta_L\rangle = \frac{1}{\sqrt{2}}\begin{pmatrix} 0 & v_L e^{i\theta_L} \\ 0 & 0 \end{pmatrix}, \quad \langle\Delta_R\rangle = \frac{1}{\sqrt{2}}\begin{pmatrix} 0 & v_R \\ 0 & 0 \end{pmatrix}, \tag{3.15}$$

$$\text{Vac. 2:}\quad \langle\phi\rangle = \frac{1}{\sqrt{2}}\begin{pmatrix} \kappa_1 & 0 \\ 0 & \kappa_2 e^{-i\theta_2} \end{pmatrix}, \quad \langle\Delta_L\rangle = \frac{1}{\sqrt{2}}\begin{pmatrix} 0 & 0 \\ v_R & 0 \end{pmatrix}, \quad \langle\Delta_R\rangle = \frac{1}{\sqrt{2}}\begin{pmatrix} 0 & 0 \\ v_L e^{i\theta_L} & 0 \end{pmatrix}, \tag{3.16}$$

As one can check, the above two minima can be transformed to each other by $U_L = U_R = i\sigma_2$ combined with the $\mathcal{P}$ parity transformation:

$$\text{Vac. 1} \xrightarrow{U_L = U_R = i\sigma_2, \&\ \mathcal{P}} \text{Vac. 2}. \tag{3.17}$$

They can also be transformed to eq. (2.10) by either $U_L = U_R = i\sigma_2$ or $\mathcal{P}$. If the potential has a minimum at eq. (2.10), then the above minima (3.15) and (3.16) also exist and have exactly the same potential depth as eq. (2.10). The vacuum of eq. (3.15) breaks $\mathrm{U}(1)_{\mathrm{em}}$ but it always coexists with the vacuum of eq. (2.10). The vacuum of eq. (3.16) generated by the parity transformation, would cause $\langle\Delta_L\rangle \gg \langle\Delta_R\rangle$ if $v_L \ll v_R$, though it does not break $\mathrm{U}(1)_{\mathrm{em}}$. Combining the transformations of both $U_L = U_R = i\sigma_2$ and parity, one can get one more vacuum with the same potential depth.

Therefore, the vacuum of eq. (2.10), if it exists, is always accompanied by several wrong vacua which have the same potential depth and are connected by discrete symmetries,[5] which are subgroups of the left-right gauge symmetry. On the other hand, if one finds a

[4] The Schur decomposition states that an arbitrary complex square matrix A can always be decomposed into $A = UTU^\dagger$, where U is a unitary matrix and T is a lower triangular matrix (i.e., $T_{ij} = 0$ for $i < j$) — see, e.g., http://mathworld.wolfram.com/SchurDecomposition.html.

[5] This may cause the cosmological domain wall problem [33] — for evading this problem, see e.g. ref. [34].

JHEP02(2019)154

minimum corresponding to one of these wrong vacua, then it implies the existence of the true vacuum. In this sense, searching for minima of these wrong types is also useful. This is particularly important for the numerical searches to be performed later.

In summary, a vacuum which superficially seems to be bad may actually imply the coexistence of a good vacuum, or may itself be a good vacuum up to some continuous symmetry transformation. Considering these possibilities, we would like to propose the following gauge independent criteria for the good vacuum:

$$\text{good vacuum criteria:} \quad \begin{array}{ll} \text{(a)} & \langle\phi\rangle \neq 0; \\ \text{(b)} & \langle\Delta_R\rangle \neq 0 \text{ or } \langle\Delta_L\rangle \neq 0; \\ \text{(c)} & \det\langle\Delta_L\rangle = \det\langle\Delta_R\rangle = 0; \\ \text{(d)} & \langle\Delta_L\rangle \neq \langle\Delta_R\rangle. \end{array} \tag{3.18}$$

For the VEV alignment in eq. (2.10), one can straightforwardly check that the above criteria are satisfied. Conversely, if a minimum of the potential satisfies eq. (3.18), the VEVs must be of the form in eq. (2.10) or can be transformed to eq. (2.10) under the previous mentioned symmetries.

4 Analytical study of LR vacua in limiting cases

In principle, we can analytically compute the first-order derivatives of the scalar potential to find out the minima. However, for the full potential in eq. (3.1) the calculations are too complicated to perform analytically. In this section, we focus on some simplified cases in which several terms in the potential are absent. Although as such it is not a full analysis (and sometimes even unrealistic), the analytical results obtained in this way provide crucial insight into the vacuum structure of the scalar potential. The details are expanded below and the results are summarized at the end of this section.

The first simplification we will make is to set α's and β's to be zero in the scalar potential (3.1) because only the α- and β-terms "lock" the bidoublet with the triplets. With $\alpha = \beta = 0$, the potential can be written as two separate parts

$$V|_{\alpha_i=\beta_j=0} = V_\phi + V_\Delta \,, \tag{4.1}$$

where V_ϕ and V_Δ contain only ϕ and $\Delta_{L/R}$ respectively. In this case, the global symmetry of the potential becomes much larger i.e. $G = [\mathrm{SU}(2)_L \otimes \mathrm{SU}(2)_R]_\phi \otimes [\mathrm{SU}(2)_L \otimes \mathrm{SU}(2)_R]_\Delta \otimes \mathrm{U}(1)_{B-L}$. (In fact this is true as long as $\alpha_3 = 0$ and $\beta_i = 0$.) Once the $\langle\phi\rangle$ and $\langle\Delta\rangle$ VEVs are switched on, the resulting symmetry will be $\mathrm{U}(1)_L \otimes \mathrm{U}(1)_R \otimes \mathrm{U}(1)_Y$. This will lead to 10 massless states out of which six will be absorbed as longitudinal modes of the gauge bosons of the theory leaving four massless states. Clearly therefore, this theory is not realistic. But nevertheless we study the vacuum structure and the symmetries of the vacuum in order to understand the same for the full model with all couplings turned on.

JHEP02(2019)154

Expressed in terms of the explicit components defined in eq. (3.7), V_ϕ and V_Δ are given by

$$\begin{aligned}
V_\phi =& -\mu_1^2(\phi_1^2+\phi_2^2) - 4\mu_2^2\phi_1\phi_2\cos\theta_2 \\
&+\lambda_1(\phi_1^2+\phi_2^2)^2 + \lambda_2 8\phi_1^2\phi_2^2\cos 2\theta_2 + \lambda_3 4\phi_1^2\phi_2^2 + \lambda_4 4\phi_1\phi_2\left(\phi_1^2+\phi_2^2\right)\cos\theta_2\,, \qquad (4.2)\\
V_\Delta =& -\mu_3^2\left[\left(a_1^2+b_1^2+c_1^2\right)+\left(a_2^2+b_2^2+c_2^2\right)\right] \\
&+\rho_1\left[\left(a_1^2+b_1^2+c_1^2\right)^2+\left(a_2^2+b_2^2+c_2^2\right)^2\right] \\
&+\rho_3\left(a_1^2+b_1^2+c_1^2\right)\left(a_2^2+b_2^2+c_2^2\right) \qquad (4.3)\\
&+\rho_2\left[4a_1^2c_1^2+b_1^4+4a_1b_1^2c_1\cos\left(\omega_1-2\omega_2+\omega_3\right)+(L\to R)\right] \\
&+\rho_4\left[4a_2b_1^2c_2\cos\left(\omega_1'-2\omega_2+\omega_3'\right)+4a_1b_2^2c_1\cos\left(\omega_1-2\omega_2'+\omega_3\right)\right. \\
&\left.\quad +8a_1a_2c_1c_2\cos\left(\omega_1-\omega_1'+\omega_3-\omega_3'\right)+2b_2^2b_1^2\cos 2\left(\omega_2-\omega_2'\right)\right].
\end{aligned}$$

To proceed, let us further set μ_2^2, λ_2, λ_4, ρ_2, and ρ_4 to zero so that we are not bothered by the cosines appearing in the above expression. In this very simplified case, we note that V_ϕ and V_Δ have essentially the same form:

$$V_{\phi 0} = -\mu_1^2(\phi_1^2+\phi_2^2)+\lambda_1(\phi_1^2+\phi_2^2)^2+4\lambda_3\phi_1^2\phi_2^2\,, \qquad (4.4)$$

$$V_{\Delta 0} = -\mu_3^2\left(\delta_1^2+\delta_2^2\right)+\rho_1\left(\delta_1^2+\delta_2^2\right)^2+(\rho_3-2\rho_1)\delta_1^2\delta_2^2\,, \qquad (4.5)$$

with $\delta_1^2 \equiv a_1^2+b_1^2+c_1^2$ and $\delta_2^2 \equiv a_2^2+b_2^2+c_2^2$. Here we have extracted $2\rho_1\delta_1^2\delta_2^2$ in eq. (4.5) so that $V_{\Delta 0}$ shows explicitly the same form as $V_{\phi 0}$. In the following discussion, we will focus on $V_{\phi 0}$ while the conclusions can be easily transferred to $V_{\Delta 0}$ by replacing $\mu_1^2 \to \mu_3^2$, $\lambda_1 \to \rho_1$ and $4\lambda_3 \to (\rho_3-2\rho_1)$.

A notable feature of $V_{\phi 0}$ is that it respects the following dihedral (D_4) symmetry

$$D_4: \begin{pmatrix}\phi_1\\ \phi_2\end{pmatrix} \to R\begin{pmatrix}\phi_1\\ \phi_2\end{pmatrix}, \quad \text{where } R=\begin{pmatrix}0 & \pm 1\\ \pm 1 & 0\end{pmatrix}, \quad \text{or } \begin{pmatrix}\pm 1 & 0\\ 0 & \pm 1\end{pmatrix}. \qquad (4.6)$$

This leads to D_4-symmetric vacuum structures shown in figure 1. The bounded from below (BFB) condition for the potential in eq. (4.4) is manifest:

$$\lambda_1 > 0, \lambda_3 > -\lambda_1\,. \qquad (4.7)$$

In the following discussion of minima, by default we assume the BFB condition should be satisfied.

From the first-order derivatives

$$\frac{\partial V_{\phi 0}}{\partial \phi_1} = 2\phi_1\left[-\mu_1^2+2\lambda_1(\phi_1^2+\phi_2^2)+4\lambda_3\phi_2^2\right]=0\,, \qquad (4.8)$$

$$\frac{\partial V_{\phi 0}}{\partial \phi_2} = 2\phi_2\left[-\mu_1^2+2\lambda_1(\phi_1^2+\phi_2^2)+4\lambda_3\phi_1^2\right]=0\,, \qquad (4.9)$$

JHEP02(2019)154

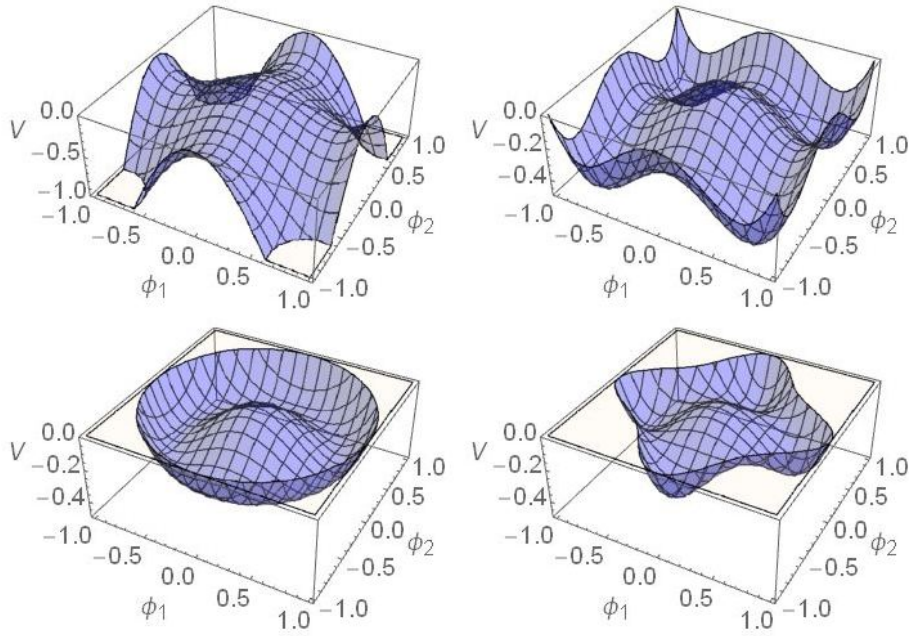

Figure 1. The D_4-symmetric potential in eq. (4.4) for different values of λ_3/λ_1. In the upper left panel ($\lambda_3/\lambda_1 = -1$), the potential is not bounded from below. In the upper right panel ($\lambda_3/\lambda_1 = -1/2$), the potential has four minima at $(\phi_1, \phi_2) = \frac{1}{\sqrt{2}}(\pm 1, \pm 1)$. In the lower left panel ($\lambda_3/\lambda_1 = 0$), the potential has infinite minima connected by an SO(2) symmetry. In the lower right panel ($\lambda_3/\lambda_1 = 1$), the potential has four minima at $(\phi_1, \phi_2) = \frac{1}{\sqrt{2}}(\pm 1, 0)$ or $\frac{1}{\sqrt{2}}(0, \pm 1)$.

we get three possible solutions

$$(\phi_1^2, \phi_2^2) = \frac{\mu_1^2}{4(\lambda_1+\lambda_3)}(1,1), \qquad \text{with } V_{\phi 0} = -\frac{\mu_1^4}{4(\lambda_1+\lambda_3)}, \tag{4.10}$$

$$(\phi_1^2, \phi_2^2) = \frac{\mu_1^2}{2\lambda_1}(0,1) \text{ or, } \frac{\mu_1^2}{2\lambda_1}(1,0), \qquad \text{with } V_{\phi 0} = -\frac{\mu_1^4}{4\lambda_1}, \tag{4.11}$$

$$(\phi_1^2, \phi_2^2) = (0,0), \qquad \text{with } V_{\phi 0} = 0. \tag{4.12}$$

Here all the denominators such as $4(\lambda_1 + \lambda_3)$ and $2\lambda_1$ are positive according to the BFB condition (4.7), which implies that the solutions (4.10) and (4.11) will not exist if $\mu_1^2 < 0$, because this will lead to negative ϕ_1^2 or ϕ_1^2. Therefore, for $\mu_1^2 < 0$, the potential has only one minimum, which is necessarily the global minimum of the potential.

By comparing the potential values $V_{\phi 0}$ of the three solutions, we can infer which one can be the global minimum without computing the second-order derivatives (Hessian matrix). One can see from eq. (4.10) and (4.11) that if $\lambda_3 > 0$ (assuming $\mu_1^2 > 0$ and $\lambda_1 > 0$), then eq. (4.11) should be the global minimum because it is deeper than the other candidates. If $\lambda_3 < 0$, eq. (4.10) is the global minimum.

Actually, one can check that if $\lambda_3 < 0$ the Hessian matrix for eq. (4.10) is positive definite while the Hessian matrix for eq. (4.11) loses positive definiteness, and vice versa. In the critical case $\lambda_3 = 0$, there is an SO(2) symmetry so any point on the circle $\phi_1^2 + \phi_2^2 = \frac{\mu_1^2}{2\lambda_1}$ is a global minimum.

JHEP02(2019)154

In summary, assuming $\mu_1^2 > 0$ and $\lambda_1 > 0$, the vacuum structure depends on the ratio λ_3/λ_1 as follows:

- $\lambda_3/\lambda_1 \leq -1$: $V_{\phi 0}$ is not BFB;
- $-1 < \lambda_3/\lambda_1 < 0$: $V_{\phi 0}$ has four minima at $(\phi_1, \phi_2) \propto (\pm 1, \pm 1)$, with equal depth;
- $\lambda_3/\lambda_1 = 0$: $V_{\phi 0}$ has infinite minima on the circle $\phi_1^2 + \phi_2^2 = \frac{\mu_1^2}{2\lambda_1}$, with equal depth;
- $\lambda_3/\lambda_1 > 0$: $V_{\phi 0}$ has four minima at $(\phi_1, \phi_2) \propto (0, \pm 1)$ and $(\pm 1, 0)$, with equal depth.

In figure 1, we show how the potential varies for different values of λ_3/λ_1. We set $\mu_1^2 = 1$ and $\lambda_1 = 1$ in eq. (4.4) and select four values -1, $-1/2$, 0, and 1 for λ_3/λ_1 so that all the four cases above are covered.

So far, we have not taken μ_2^2, λ_2, λ_4 into consideration. In the presence of these terms, the D_4 symmetry will be broken and the complexity of the above analysis will be increased. We do not plan to derive the corresponding analytic expressions. But we can discuss qualitatively the consequences using the D_4-symmetric conclusions. If we set $\mu_2^2 > 0$ while keeping λ_2 and λ_4 still at zero, this is the same as adding the term $-4\mu_2^2\phi_1\phi_2\cos\theta_2$ to the D_4-symmetric potential $V_{\phi 0}$. From the potential $V_{\phi 0} - 4\mu_2^2\phi_1\phi_2\cos\theta_2$ we can immediately see that $\cos\theta_2$ should be 1 (if $4\mu_2^2\phi_1\phi_2 > 0$) or -1 (if $4\mu_2^2\phi_1\phi_2 < 0$) to reach a minimum, which implies that we would still get real solutions even if we turn on the complex phase. Therefore instead of $V_{\phi 0} - 4\mu_2^2\phi_1\phi_2\cos\theta_2$ we can focus on $V_{\phi 0} - 4\mu_2^2\phi_1\phi_2$. In figure 2, we plot both $V_{\phi 0}$ and $V_{\phi 0} - 4\mu_2^2\phi_1\phi_2$ to show the changes caused by the μ_2^2 term. In the upper left panel ($\lambda_3/\lambda_1 = -1/2$, $\mu_2^2 = 0$), the four minima have the same depth due to the D_4 symmetry. When the μ_2^2 term is added (for illustration we choose $\mu_2^2 = 0.15$), as shown in the corresponding lower panel, two of the minima become deeper than the other two. Note that in this case (ϕ_1, ϕ_2) at the minima still align in the direction (1, 1) or (1, -1). In the middle panels ($\lambda_3/\lambda_1 = 0$), the SO(2) symmetry is broken when μ_2 is nonzero, leading also to the VEV alignment $(\phi_1, \phi_2) \propto (1, 1)$. In the right panels ($\lambda_3/\lambda_1 = 1$), the four minima still have equal depth after adding the μ_2^2 term, but the VEV alignment is changed from (1, 0) or (0, 1) to (1, r) or (r, 1) where r depends on μ_2.

Therefore, within the simple D_4-soft-broken potential $V_{\phi 0} - 4\mu_2^2\phi_1\phi_2\cos\theta_2$, we can already get an arbitrary VEV alignment $(\phi_1, \phi_2) \propto (1, r)$. Further turning on λ_2 and λ_4 couplings may produce more possibilities (e.g. spontaneous CP breaking) which should include the VEV alignments obtained in $V_{\phi 0} - 4\mu_2^2\phi_1\phi_2\cos\theta_2$.

Now let us discuss the triplet sector. As previously mentioned, if $\rho_2 = \rho_4 = 0$, the potential of Δ_L and Δ_R reduces to $V_{\Delta 0}$ which has the same form as $V_{\phi 0}$. Using the previous conclusions on $V_{\phi 0}$, we know that when

$$\mu_3^2 > 0, \rho_3 > 2\rho_1 > 0\,, \tag{4.13}$$

the D_4-symmetric potential $V_{\Delta 0}$ has four minima at $(\delta_1, \delta_2) \propto (0, 1)$ or $(1, 0)$, which implies the VEV alignment

$$\langle \Delta_L \rangle = 0, \langle \Delta_R \rangle \neq 0 \tag{4.14}$$

can be obtained.

JHEP02(2019)154

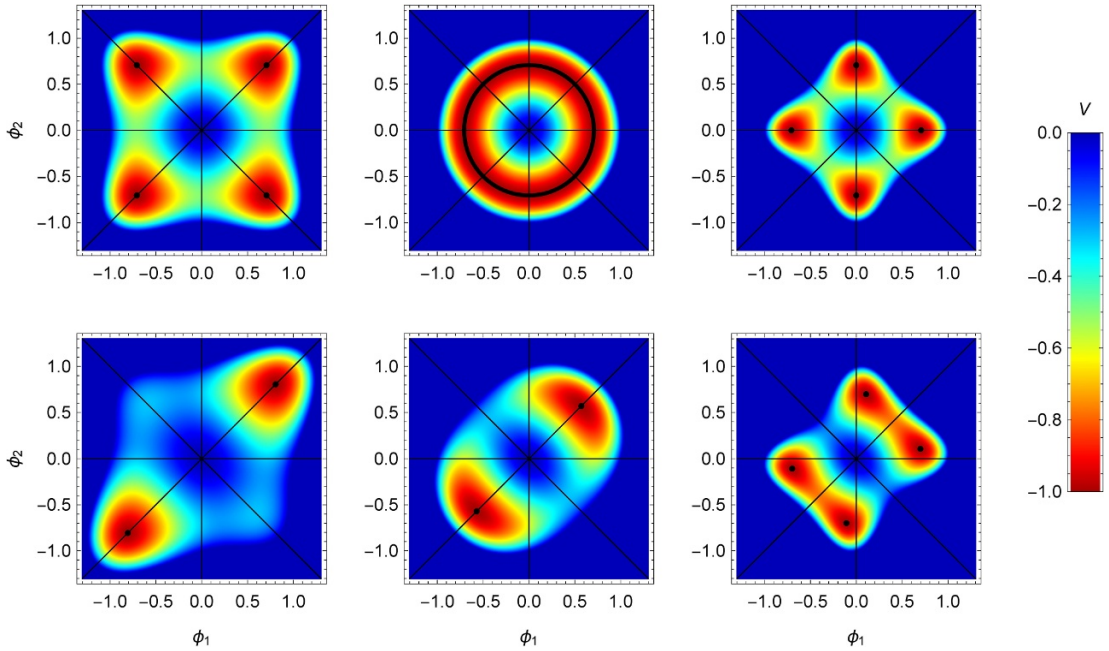

Figure 2. Vacua in the D_4-symmetric (upper panels) and D_4-broken (lower panels) potentials. The D_4-symmetric potential is given by eq. (4.4) with $\lambda_3 = -1/2$, 0, and 1 (from left to right) and $\mu_1^2 = \lambda_1 = 1$. The D_4-broken potential is obtained by adding $-4\mu_2^2\phi_1\phi_2$ to eq. (4.4) with $\mu_2^2 = 0.15$. This changes the locations of stable vacua (marked in black). The potentials are normalized so that $V_{\min} = -1$.

We would like to point it out that even if ρ_2 and ρ_4 are nonzero, V_Δ is still D_4-symmetric. The symmetry transformation is similar to eq. (4.6) with (ϕ_1, ϕ_2) replaced by (Δ_L, Δ_R). Consequently, the VEV alignments of (Δ_L, Δ_R) from eq. (4.4) have only three possibilities: (i) one of (Δ_L, Δ_R) is nonzero and the other is zero, like eq. (4.14); (ii) both are zero; or (iii) both are nonzero but $\Delta_L = \Delta_R$.

However, the above arguments treat Δ_L and Δ_R as two singlets and do not take into consideration the fact that they have internal components. Analyses in terms of the components (a_i, b_i, c_i) will be much more complicated. We adopt a numerical method to check the above conclusions and find that there are indeed only the three cases, except that (iii) should be interpreted as $a_1^2 + b_1^2 + c_1^2 = a_2^2 + b_2^2 + c_2^2$.

Besides, one should notice that for nonzero ρ_2 and ρ_4, eq. (4.13) is no longer the condition to get eq. (4.14). But at least the simple conclusion with $\rho_2 = \rho_4 = 0$ is enough to show that the VEV alignment in eq. (4.14) can be obtained in a part of the parameter space.

Eq. (4.14) is what we need to achieve spontaneous parity breaking. The other two possible cases, namely $\Delta_L = \Delta_R \neq 0$ and $\Delta_L = \Delta_R = 0$, can be modified by D_4-breaking terms [e.g. the α and β terms in (3.1)] so that $\Delta_L \neq \Delta_R$ and $\Delta_R \neq 0$. However the experimental constraints require that $\langle\Delta_L\rangle$ should be much smaller than $\langle\Delta_R\rangle$ since the former, limited by the electroweak ρ parameter, has to be lower than the GeV scale while the latter should be above the TeV scale to satisfy the collider bounds on W_R. Such a

JHEP02(2019)154

strong hierarchy would require substantial fine-tuning in the scalar potential. Therefore, the solution $\langle \Delta_L \rangle = 0$ as a consequence of symmetry is a more favored option.

Focused on the solution with zero Δ_L and nonzero Δ_R, we proceed to study the VEV alignments of the internal components of Δ_R. For simplicity, let us first set $\rho_4 = 0$ (μ_3^2, ρ_1, ρ_2, and ρ_3 are nonzero). Note that in the remaining terms of V_Δ, only the ρ_3 term couples Δ_L to Δ_R. This term has no contribution to the first-order derivatives at the minimum with zero Δ_L because

$$\frac{\partial(\delta_1^2\delta_2^2)}{\partial a_i} = \frac{\partial(\delta_1^2\delta_2^2)}{\partial b_i} = \frac{\partial(\delta_1^2\delta_2^2)}{\partial c_i} = 0, \quad \text{for } \Delta_L = 0.$$

In the absence of ρ_3 and ρ_4, Δ_R decouples with Δ_L in V_Δ. Hence we only need to consider the following part of the potential

$$\begin{aligned} V_{\Delta 2} &= -\mu_3^2\left(a_2^2{+}b_2^2{+}c_2^2\right){+}\rho_1\left(a_2^2{+}b_2^2{+}c_2^2\right)^2{+}\rho_2\left[4a_2^2c_2^2{+}b_2^4{+}4a_2b_2^2c_2\cos\left(\omega_1'{-}2\omega_2'{+}\omega_3'\right)\right] \\ &= -\mu_3^2\delta_2^2{+}\rho_1\delta_2^4{+}4\rho_2|\det\Delta_R|^2\,, \end{aligned} \tag{4.15}$$

where in the second line we have simplified the ρ_2 term which can be verified by an explicit computation. To proceed, we need the following useful relation:

$$0 \le |\det\Delta_R| \le \frac{1}{2}\delta_2^2\,, \tag{4.16}$$

which can be proven by

$$\delta_2^2 = a_2^2 + b_2^2 + c_2^2 \ge \max(b_2^2 + 2a_2c_2, b_2^2 - 2a_2c_2) \ge |b_2^2 + 2a_2c_2e^{i\omega'}| = 2|\det\Delta_R|\,, \tag{4.17}$$

where $\omega' = \omega_1' - 2\omega_2' + \omega_3'$. Note that for a fixed value of δ_2^2, $|\det\Delta_R|$ can reach any value in the above range. Therefore, we can parametrize $|\det\Delta_R|$ as $\frac{1}{2}\delta_2^2\cos\theta$ and write

$$V_{\Delta 2} = -\mu_3^2\delta_2^2 + \left(\rho_1 + \rho_2\cos^2\theta\right)\delta_2^4\,. \tag{4.18}$$

From eq. (4.18), it is obvious to identify the minima. Let us take $\rho_1 > 0$ and $\mu_3^2 > 0$, which is necessary to satisfy the BFB condition and obtain nonzero VEVs. If $\rho_2 > 0$, the minimum should be at $\cos^2\theta = 0$; and if $\rho_2 < 0$, it should be at $\cos^2\theta = 0$. Therefore the minima of $V_{\Delta 2}$ should locate at:

$$\rho_2 > 0: \qquad \delta_2^2 = \frac{\mu_3^2}{2\rho_1}\,, \qquad \det\Delta_R = 0, \tag{4.19}$$

$$\rho_2 < 0: \qquad \delta_2^2 = \frac{\mu_3^2}{2(\rho_1+\rho_2)}, \qquad \det\Delta_R = \frac{1}{2}\delta_2^2 = \frac{\mu_3^2}{4(\rho_1+\rho_2)}\,. \tag{4.20}$$

As long as $\alpha_{1,2,3} = \beta_{1,2,3} = 0$, we always have the freedom to transform $\Delta_R \to U_R\Delta_R U_R^\dagger$ individually (without the corresponding transformation of the bidoublet ϕ) within the triplet potential V_Δ. Again, according to the Schur decomposition, we can always transform Δ_R to a lower triangular matrix. In this form, eqs. (4.19) and (4.20) should be

$$\rho_2 > 0: \qquad \Delta_R = \sqrt{\frac{\mu_3^2}{2\rho_1}}\begin{pmatrix} 0 & 0 \\ 1 & 0 \end{pmatrix}, \tag{4.21}$$

$$\rho_2 < 0: \qquad \Delta_R = \sqrt{\frac{\mu_3^2}{4(\rho_1+\rho_2)}}\begin{pmatrix} 1 & 0 \\ 0 & -1 \end{pmatrix}. \tag{4.22}$$

JHEP02(2019)154

Eq. (4.21) is straightforward to get, because if $\det \Delta_R = 0$, only the 2–1 element can be nonzero. Eq. (4.22) has zero a_2 because when $|\det \Delta_R| = \frac{1}{2}\delta_2^2$, $|a_2|$ and $|c_2|$ should be equal, according to the derivation of eq. (4.16). One should keep in mind that eqs. (4.21) and (4.22) are derived under the assumption that $\mu_3^2 > 0$, $\rho_4 = \alpha_{1,2,3} = \beta_{1,2,3} = 0$, and that the potential is BFB.

The above analyses implies the following *sufficient but not necessary* conditions to get a good vacuum:

$$\mu_1^2, \mu_2^2, \mu_3^2 > 0, \tag{4.23}$$

$$\lambda_1 > 0, \lambda_2 = 0, \lambda_3 > -\lambda_1, \lambda_4 = 0, \tag{4.24}$$

$$\rho_1 > 0, \rho_2 > 0, \rho_3 > 2\rho_1, \rho_4 = 0, \tag{4.25}$$

$$\alpha_{1,2,3} = \beta_{1,2,3} = 0. \tag{4.26}$$

If the potential parameters satisfy the above conditions, then it can be guaranteed that the potential has a global minimum corresponding to a good vacuum. However, in practice, α_i and β_i cannot all be set to zero because of additional massless states, as mentioned before. To solve this problem, we can add small perturbations to α_i to avoid the massless states. More explicitly, using the above condition, we can easily find a set of potential parameters satisfying eqs. (4.23), (4.24) and (4.25). Then if we set α_i to zero, the potential has a good vacuum, though not realistic. Next we can explore the parameter space around this point by tentatively adding some small perturbations to α_i. If the perturbations are small enough, the conclusion should hold as well. Sometimes, the perturbations can be very large without changing the conclusion. The exploration starting from eq. (4.26) needs numerical assistance, as will be done in section 5. And we will show (see figure 5), indeed one can find some deviations from eq. (4.26) that lead to successful symmetry breaking.

We have a few additional comments on the above conditions:

- The above conditions also guarantee BFB, whereas the converse is not necessarily true.
- If $-\lambda_1 < \lambda_3 < 0$, $\langle\phi\rangle \propto \mathrm{diag}(1,1)$. If $0 < \lambda_3$, $\langle\phi\rangle \propto \mathrm{diag}(1,r)$ with $r \neq 1$;
- The vacuum obtained in this way always has $\langle\Delta_L\rangle = 0$.

The conditions (4.23)–(4.26) obtained by the above analytic study will be very useful in the subsequent numerical study. It helps to quickly find out a viable region in which the potential has a good vacuum. In addition, it is also important for setting some benchmarks when studying the global minimum constraints.

Here we would like to comment on the influence of including higher dimensional operators on our results. Taking $\Lambda^{-2}[\mathrm{Tr}(\Delta_R^\dagger \Delta_R)]^3$ as an example, we expect that Λ is much higher than all VEVs. Let us denote the original potential as V and the new term as δV. Assuming V has a minimum with $\langle\Delta_R\rangle$ given in eq. (2.10), then we have $\partial V/\partial\Delta_R = 0$ at $(\delta_R^0, \delta_R^+, \delta_R^{++}) = (v_R/\sqrt{2}, 0, 0)$. This implies that the potential V at the local scale essentially has a negative mass term for δ_R^0, and positive mass terms for the other two components, if the other fields ϕ and Δ_L are replaced by their VEVs. Now including δV,

JHEP02(2019)154

this scenario would not be changed if the new contribution is small, which is expected since Λ is relatively high. A full study of all possible higher dimensional operators is out of the scope of this work. But at least one can draw the conclusion that including some of them with relatively high Λ would not change the results significantly.

In this paper we have focused on the tree level potential without including radiative corrections, which are expected to be generally small if the couplings are in the perturbative region. Similar to the above arguments on higher dimensional operators, these small corrections can only adjust the nonzero VEV slightly while zero VEVs remain stable, as long as the loop corrections do not flip the positiveness of any quadratic term. Including large radiative corrections may have interesting consequences which will be further elsewhere.

5 Numerical study

With the modern technology of numerical computation, given a set of specific values of the potential parameters one can readily obtain a numerical minimum. There have been various algorithms well developed to find minima of multi-variable functions.[6] Most algorithms are based on iterative searches which means the program starts from a given initial point and iteratively computes the next step according to some principles until the steps converge to a minimum. The convergence can not be guaranteed, so for a single process searching for minima there is a small probability of failure. In case of failure, one can try to start the process again with a different initial point. Repeating the processes will eventually arrive at a minimum which may be local or global.

Once we get a numerical minimum of the potential, we can inspect the field component values at the minimum, checking if some of them are zero or some of them are equal. However, in numerical calculations it is impossible to have infinite accuracy so the would-be zero numbers are generally nonzero but very small (e.g. $\sim 10^{-9}$ for numerical minimization based on a 8-byte real number system). This implies that, due to limited accuracy, there is no absolute equality in the numerical results. The simplest solution to this problem is by setting a cut on the difference of two numbers, below which the two numbers are thought to be equal and above which they are not.[7] But this may cause misjudgment since the difference of two actually unequal numbers may occasionally be smaller than the cut. To double check if a field component is zero at the minimum, we can invoke the minimization process again with this component fixed to zero. If it gives a slightly better minimization, then we can conclude that it is zero at the minimum.

We apply the above numerical method to the LRSM potential in eq. (3.1). First, let us arbitrarily set the values of potential parameters to see in general what VEV alignments would be obtained. Both the quadratic and quartic couplings are generated by a uniform distribution in the interval $[-4\pi, 4\pi]$. In this work, the energy scales of all dimensional quantities such as the quadratic couplings and the field values are not relevant.

[6] See, e.g. [71] or the `SciPy` document: https://docs.scipy.org/doc/scipy/reference/generated/scipy.optimize.minimize.html#scipy.optimize.minimize. In this paper, we adopt the Nelder-Mead simplex method which is the most commonly used algorithm since it does not require derivatives of the function.

[7] Actually, we use this to check whether a quantity is zero while for checking whether two quantities a and b are equal, we convert it to the problem of checking whether $(a-b)/b$ is zero.

JHEP02(2019)154

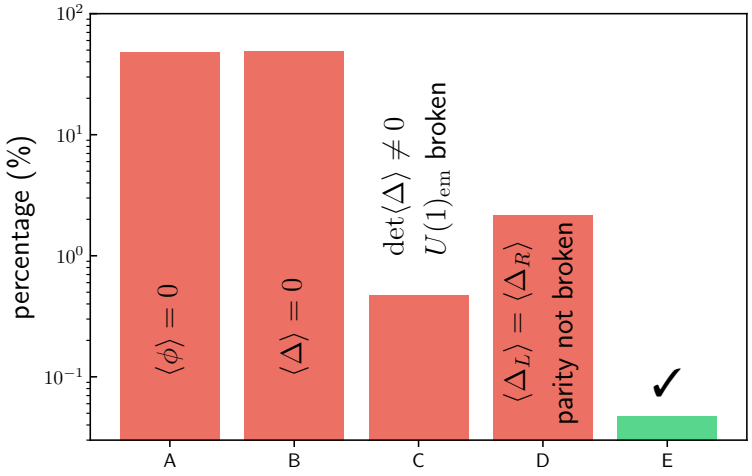

Figure 3. Pecentages of the samples leading to the five types of vacua (type A: 48.6%, type B: 48.7%, type C: 0.5%, type D: 2.2%, type E: 0.05%) classified by the conditions in eq. (3.18). Only type E corresponds to viable symmetry breaking of LRSM. More details of the five types of VEV alignments are listed in table 1. To generate the samples, we randomly set the potential parameters in eq. (3.1), check the BFB condition, and numerically minimize the potentials.

For example, we can use $v \equiv 246\,\text{GeV}$ as the energy unit, instead of GeV or TeV, then $\mu_1^2 = 0.5 \times (246\ \text{GeV})^2 = 0.5v^2$ can be simply written as 0.5 in the computer program.

The quartic couplings generated in the above way can not guarantee that the potential is BFB. The BFB check can be numerically performed by setting the quadratic couplings to zero and then run the minimization process. If any point with $V < 0$ is reached during minimization, then the potential is not BFB and the sample is abandoned. If a sample passes the BFB check, then we further minimize the potential with the nonzero quadratic couplings.

When a minimum is successfully obtained in this process, we check if it violates the four good vacuum conditions in eq. (3.18), from (a) to (d) sequentially. If any of them is violated, then we stop checking the remaining conditions and tag it as type A, B, C, or D, corresponding to the violation of condition (a), (b), (c), or (d), respectively. If all the conditions are satisfied, it is tagged as type E, a good and successful vacuum.

In figure 3, we present the result of the above analysis on 144891 samples (all passing the BFB check). In this randomly generated data set, 70380, 70625, 683, and 3135 of the samples fall into the categories of type A, B, C, and D, respectively. Only 68 samples are of type E, which is about 0.05% of the total number. We further inspect the VEV alignments of all samples of the five types and list them in table 1. As we have discussed in section 3.2, some symmetry transformations can transform the VEV alignments from one form to another — see, e.g. eq. (3.17). For such cases, in table 1 we only list the representative forms. More specifically, whenever appropriate U_L and U_R transformations are allowed (e.g. $\langle\phi\rangle = 0$, or $\kappa_1 = \kappa_2$, or $U_L = U_R = i\sigma_2$), we always use them to transform Δ_L and Δ_R to lower triangular forms according to the Schur decomposition.

The low percentage (0.05%) of type E can be understood from the analytical studies in section 4. First, for those simplified cases we have studied, one can see that the quadratic

JHEP02(2019)154

type	definition	$\langle\phi\rangle$	$\langle\Delta_L\rangle$	$\langle\Delta_R\rangle$
A	violates eq. (3.18) condition (a) $\langle\phi\rangle = 0$	$\begin{bmatrix} 0 & 0 \\ 0 & 0 \end{bmatrix}$	$\begin{bmatrix} 0 & 0 \\ c_1 & 0 \end{bmatrix}$	$\begin{bmatrix} 0 & 0 \\ c_1 & 0 \end{bmatrix}$
		$\begin{bmatrix} 0 & 0 \\ 0 & 0 \end{bmatrix}$	$\begin{bmatrix} c_1 & 0 \\ 0 & -c_1 \end{bmatrix}$	$\begin{bmatrix} c_1 & 0 \\ 0 & -c_1 \end{bmatrix}$
		$\begin{bmatrix} 0 & 0 \\ 0 & 0 \end{bmatrix}$ $\cdots$	$\begin{bmatrix} 0 & 0 \\ 0 & 0 \end{bmatrix}$ $\cdots$	$\begin{bmatrix} 0 & 0 \\ 0 & 0 \end{bmatrix}$ $\cdots$
B	violates eq. (3.18) condition (b) $\langle\Delta_L\rangle = \langle\Delta_R\rangle = 0$	$\begin{bmatrix} c_1 & 0 \\ 0 & c_1 \end{bmatrix}$	$\begin{bmatrix} 0 & 0 \\ 0 & 0 \end{bmatrix}$	$\begin{bmatrix} 0 & 0 \\ 0 & 0 \end{bmatrix}$
		$\begin{bmatrix} c_1 & 0 \\ 0 & c_3 \end{bmatrix}$	$\begin{bmatrix} 0 & 0 \\ 0 & 0 \end{bmatrix}$	$\begin{bmatrix} 0 & 0 \\ 0 & 0 \end{bmatrix}$
C	violates eq. (3.18) condition (c) $\det\langle\Delta_L\rangle$ or $\det\langle\Delta_R\rangle \neq 0$	$\begin{bmatrix} c_1 & 0 \\ 0 & c_1 \end{bmatrix}$	$\begin{bmatrix} c_2 & 0 \\ 0 & -c_2 \end{bmatrix}$	$\begin{bmatrix} c_2 & 0 \\ 0 & -c_2 \end{bmatrix}$
		$\begin{bmatrix} c_1 & 0 \\ 0 & c_3 \end{bmatrix}$ $\cdots$	$\begin{bmatrix} c_2 & 0 \\ 0 & -c_2 \end{bmatrix}$ $\cdots$	$\begin{bmatrix} c_2 & 0 \\ 0 & -c_2 \end{bmatrix}$ $\cdots$
D	violates eq. (3.18) condition (d) $\langle\Delta_L\rangle = \langle\Delta_R\rangle$	$\begin{bmatrix} c_1 & 0 \\ 0 & c_3 \end{bmatrix}$	$\begin{bmatrix} 0 & 0 \\ c_2 & 0 \end{bmatrix}$	$\begin{bmatrix} 0 & 0 \\ c_2 & 0 \end{bmatrix}$
E	satisfies eq. (3.18)	$\begin{bmatrix} c_1 & 0 \\ 0 & c_2 \end{bmatrix}$	$\begin{bmatrix} 0 & 0 \\ c_3 & 0 \end{bmatrix}$	$\begin{bmatrix} 0 & 0 \\ c_4 & 0 \end{bmatrix}$

Table 1. VEV alignments of various types of minima found in the numerical search. Except for type E, each type is defined by a relation that violates the good vacuum conditions in eq. (3.18). The typical VEV alignments in each type are listed in the 3rd–5th columns, with "c_i" ($i = 1, 2, 3, 4$) standing for independent nonzero values. Note that other VEV alignments that can be converted to the ones in this table are not shown (see the main text for more details about this issue), and "$\cdots$" indicates that the enumeration is not exhaustive.

JHEP02(2019)154

couplings $\mu^2_{1,2,3}$ have to be positive to get nonzero $\langle\phi\rangle$ and $\langle\Delta_{L,R}\rangle$. Let us assume that for more general potentials (e.g. with λ_4, $\beta_{1,2,3}$ nonzero) this conclusion approximately holds as well. Then requiring the three quadratic couplings to be positive in the random number generation already produces a factor of $(1/2)^3 = 1/8$ which suppresses the percentage by one order of magnitude. Moreover, in eq. (4.24) and eq. (4.25) some quartic couplings may also need to be positive to get a good vacuum. If 11 of the 17 parameters in the full potential are required to be positive, the suppression factor can easily reach $(1/2)^{11} \approx 0.05\%$. Some parameters may contribute suppression factors smaller or larger than $1/2$, say $1/p$. Generally it is possible to get a significant suppression at the order of $(1/p)^n$ where $n \leq 17$. This explains why the percentage can be suppressed to the level of 0.05%.

Although the suppression is understandable, it is would be better to avoid the suppression or at least to know a part of the parameter space that would lead to the correct symmetry breaking with a much higher probability. According to our analytical study, we are led to simple conditions to enhance the probability of ending up in a good vacuum:

$$\begin{aligned}
&0 \leq \mu_i^2 \leq 4\pi v^2 && (i = 1,\, 2,\, 3),\\
&0 \leq \lambda_i, \rho_i \leq 4\pi && (i = 1,\, 2,\, 3,\, 4),\\
&0 \leq \alpha_i \leq 0.2\pi && (i = 1,\, 2,\, 3),\\
&\beta_i = 0 && (i = 1,\, 2,\, 3).
\end{aligned} \tag{5.1}$$

Requiring the additional constraints in eq. (5.1), we repeat the numerical process used to generate figure 3 and obtain the left plot in figure 4. As the plot shows, with these constraints, the percentage of type E is enhanced to 16.2%, which is at the same order of magnitude as the other types. Eq. (5.1) is proposed based on the analytical result summarized in eqs. (4.23)–(4.26), but it allows more general parameter settings, e.g. λ_2, $\rho_{2,4}$, $\alpha_{1,2,3}$ do not have to be fixed to zero. It is a compromise between the generality (also simplicity) and the enhancement of the percentage of good vacuum solutions.

Including more constraints from eqs. (4.23)–(4.26) can further enhance the percentage at the cost of loss of generality. In the right panel of figure 4, we include the constraints

$$\lambda_2 = \lambda_4 = \rho_4 = 0, \qquad \rho_3 > 2\rho_1, \tag{5.2}$$

together with eq. (5.1) and obtain a much higher percentage (86%) of type E, which means the majority of the samples generated under these constraints have good vacua.

We also note that figure 3 and figure 4 establish our claim in the introduction that the BFB conditions only provide a necessary but not sufficient condition for an acceptable vacuum since all the columns in figure 3 and figure 4 satisfy the BFB condition whereas only the green column satisfies the desired vacuum condition.

5.1 Global minimum constraints

As we have seen that among those randomly generated samples some may have type E vacua and some may not, if the potential is required to lead to successful symmetry breaking, it must be subjected to a lot of constraints. Below we would like to study such constraints.

JHEP02(2019)154

Note that these constraints are not fully equivalent to the requirement that the potential has a type E minimum. If the potential has no type E minimum, then of course it can not lead to successful symmetry breaking. But even if it has a type E minimum, the minimum could be a local one which coexists with other much deeper minima. Then the vacuum at the type E minimum is not absolutely stable as it may decay to other deeper vacua via quantum tunneling or thermal fluctuation. There is a possibility that the decay rate is very low so that the lifetime is longer than the age of the Universe, known as the meta-stability. Since the analyses including meta-stability would be too much involved here, for simplicity, we only consider the absolute stability. Therefore in what follows, when we claim that a potential can lead to successful symmetry breaking, we mean the potential has a global minimum of type E. The corresponding constraints will be referred to as *the global minimum constraints*.

Let us investigate the effect of global vs. local minimum. Since there is no minimization algorithm that can guarantee to find global minima for general cases, the method of global minimum test used in our program is repeating the minimization process with random initial values for many times. If none of these minima is deeper than the one being tested, then more likely it is a global minimum. Obviously the more times the process is repeated, the more likely it is a global minimum. This method still can not guarantee the correctness of the global minimum, but with a large number of repetitions, the result will be statistically reliable. To quantify the effect of testing for a global minimum, we present the constraints on the six parameters $\alpha_{1,2,3}$ and $\beta_{1,2,3}$ as illustration in figure 5, where the green region has successful symmetry breaking with a global minimum, while the blue region only is a global minimum. Each plot shows the constraint on a pair of the parameters ($\alpha_i - \alpha_j$ or $\beta_i - \beta_j$) while the other parameters are fixed at a chosen benchmark point:

$$\text{benchmark:} \begin{cases} (\mu_1^2, \mu_2^2, \mu_3^2) = (5.0, 2.0, 9.0)v^2\,, \\ (\lambda_1, \lambda_2, \lambda_3, \lambda_4) = (1.0, 0.0, 1.2, 0.0)\,, \\ (\rho_1, \rho_2, \rho_3, \rho_4) = (1.0, 0.2, 3.0, 0.0)\,, \\ (\alpha_1, \alpha_2, \alpha_3) = (0.5, 0.0, 0.7)\,, \\ (\beta_1, \beta_2, \beta_3) = (0.0, 0.0, 0.0)\,. \end{cases} \tag{5.3}$$

This benchmark is set in such a way that by default (i.e. no parameters are changed) it has a global minimum of type E. The plots are produced in coarse grids because for each sample the program has to run the global minimum test for many times which is CPU intensive. So currently we cannot compute too many samples with limited computer power and consequently the interval of grid scan cannot be too small. In figure 5 we use 40×40 grids in the range $[-4\pi, 4\pi]^2$ with a interval of 0.2π.

As one can see in the left panels of figure 5, the green regions cover the central point $\alpha_{1,2,3} = 0$ and the nearby part (within 3 or 4 blocks) is also green. This implies that small α_i indeed can lead to absolutely stable type E vacua, which is a conjecture of our analytical study. This is approximately true also for the β_i parameters. However, the difference is that the α_i do not have to be small (in some direction they can reach 4π) while the β_i, at least for this benchmark, have to be small.

JHEP02(2019)154

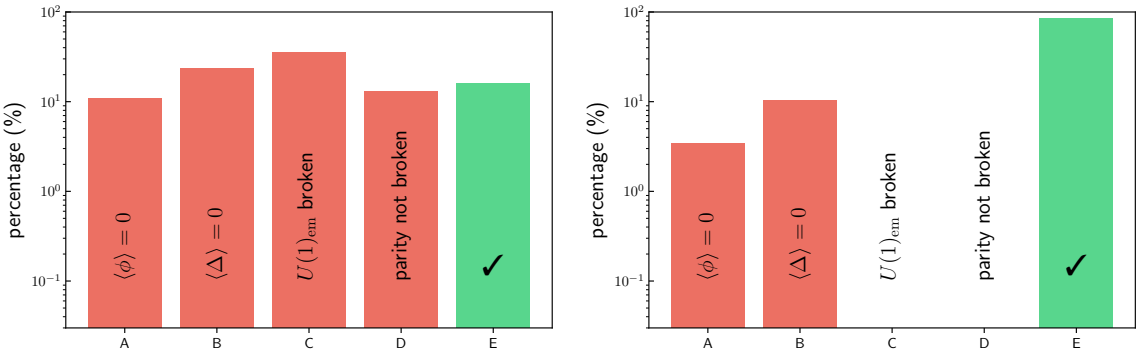

Figure 4. Similar to figure 3 except that the potential parameters are generated with additional constraints given by eq. (5.1) and eq. (5.2) so that the probability of obtaining type E vacua is significantly enhanced. *Left*: all potential parameters are positive, $\alpha_{1,2,3}$ are suppressed by a small factor and $\beta_{1,2,3} = 0$. The percentages are 11.0% (A), 23.9% (B), 35.9% (C), 13.0% (D), 16.2% (E). *Right*: in addition to the constraints used in the left panel, we require that $\lambda_2 = \lambda_4 = \rho_4 = 0$, $\rho_3 > 2\rho_1$. The percentages are 3.4% (A), 10.5% (B), 0 (C), 0 (D), 86.0% (E).

5.2 Constraints on scalar masses

Because the scalar mass spectrum is fully determined by the parameters of the scalar potential, the global minimum constraints on the potential parameters can be converted to constraints on the scalar mass spectrum. After symmetry breaking the scalar sector contains (including the Goldstone bosons) eight electrically neutral bosons, four singly charged bosons and two doubly charged bosons, among which the bosons with the same electric charge generally have mass mixing. Therefore the mass matrices of the neutral and singly charged scalar bosons are quite complicated, but the mass matrix of doubly charged bosons is much simpler. For simplicity, we will thus only discuss the mass spectrum of the doubly charged bosons. Their mass matrix is

$$\mathcal{M}_{11}^{\pm\pm} = \begin{pmatrix} \mathcal{M}_{11}^{\pm\pm} & \mathcal{M}_{12}^{\pm\pm} \\ \mathcal{M}_{21}^{\pm\pm} & \mathcal{M}_{22}^{\pm\pm} \end{pmatrix}, \tag{5.4}$$

where

$$\mathcal{M}_{11}^{\pm\pm} = \frac{1}{2}(\rho_3 - 2\rho_1)v_R^2 + 2\rho_2 v_L^2 + \frac{1}{2}\alpha_3(\kappa_1^2 - \kappa_2^2)\,, \tag{5.5}$$

$$\mathcal{M}_{22}^{\pm\pm} = 2\rho_2 v_R^2 + \frac{1}{2}(\rho_3 - 2\rho_1)v_L^2 + \frac{1}{2}\alpha_3(\kappa_1^2 - \kappa_2^2)\,, \tag{5.6}$$

$$\mathcal{M}_{12}^{\pm\pm} = \left(\mathcal{M}_{21}^{\pm\pm}\right)^* = 2\rho_4 v_R v_L e^{-i\theta_L} + \frac{1}{2}\left(\beta_1\kappa_1\kappa_2 e^{-i\theta_2} + \beta_2\kappa_2^2 e^{-2i\theta_2} + \beta_3\kappa_1^2\right). \tag{5.7}$$

Note that if ρ_4 and $\beta_{1,2,3}$ are set to zero, then the mass matrix is diagonal and one can immediately obtain the eigenvalues (i.e. the mass squares of the two doubly charged bosons):

$$\left(M_1^{\pm\pm}\right)^2 = (\rho_3 - 2\rho_1)v_R^2/2 + \alpha_3(\kappa_1^2 - \kappa_2^2)/2\,, \tag{5.8}$$

$$\left(M_2^{\pm\pm}\right)^2 = 2\rho_2 v_R^2 + \alpha_3(\kappa_1^2 - \kappa_2^2)/2\,. \tag{5.9}$$

JHEP02(2019)154

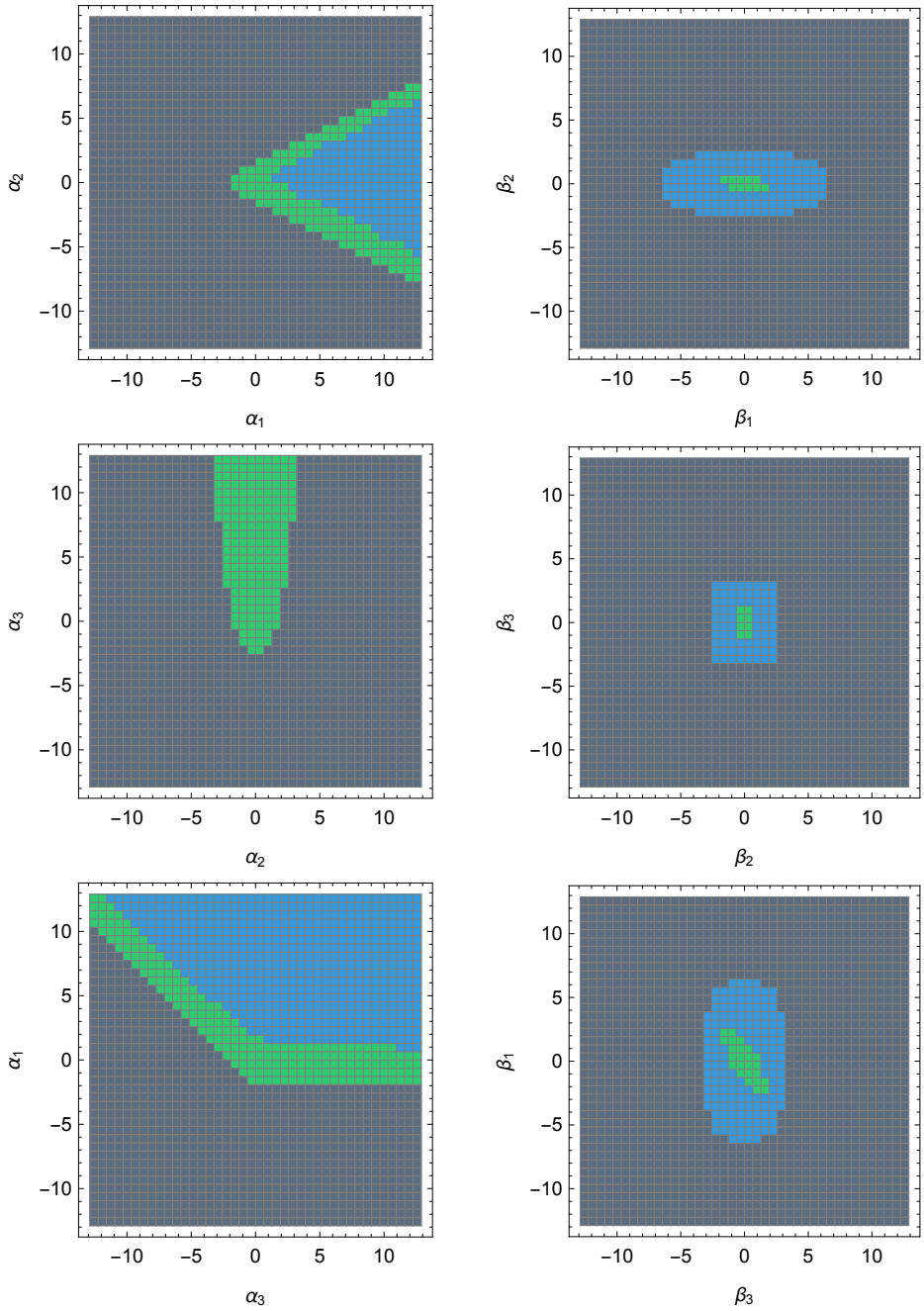

Figure 5. Global minimum constraints on α_i and β_i. Samples in the green region have type E global minima so they will lead to successful symmetry breaking; the blue region violates the global minimum constraints which means that either the potential does not have type E minimum or its type E minimum is local; the black region violates the BFB condition. Other potential parameters, if not indicated by the plots, are fixed at the benchmark values in eq. (5.3). The grid interval is 0.2π.

JHEP02(2019)154

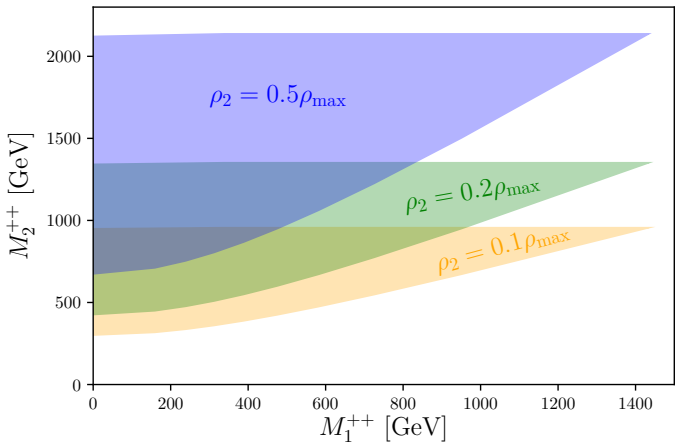

Figure 6. The global minimum constraint on the two doubly charged scalar masses $(M_1^{\pm\pm}, M_2^{\pm\pm})$ for the benchmark point given by eq. (5.10).

This greatly simplifies the scenario and we would like to take it as an example to show the global minimum constraints on the mass spectrum. We also set other parameters to the following specific values:

$$\begin{aligned}(\mu_1^2, \mu_2^2, \mu_3^2) &= (0.3, 0.2, 9)v_X^2,\\ (\lambda_1, \lambda_2, \lambda_3, \lambda_4) &= (0.13, 0, 0.6, 0),\\ (\alpha_1, \alpha_2, \alpha_3) &= (0, 0, 1\times 10^{-4}),\end{aligned} \tag{5.10}$$

except for ρ_1, ρ_2 and ρ_3. We take ρ_1 and ρ_3 as free parameters ranging from $-\rho_{\max}$ to $\rho_{\max}$, and fix ρ_2 at some values indicated in figure 6. Here $\rho_{\max}$ is set at a small value 10^{-3} (for a reason to be explained below) and v_X^2 is a floating energy scale which is always tuned to make $\sqrt{\kappa_1^2 + \kappa_2^2} = 246\,\text{GeV}$.

To make the scenario considered here more realistic, we also require that it contains a SM-like Higgs boson with the mass $m_h \approx 125\,\text{GeV}$ and a large v_R so that the mass of W_R is above the LHC constraints. The parameters in eq. (5.10) have been tuned in such a way that for ρ_1 and ρ_3 varying in $[-\rho_{\max}, \rho_{\max}]$, the SM Higgs mass m_h ranges within $125\pm1.5\,\text{GeV}$ and v_R ranges from 21 to 67 TeV. We have checked that changing $\rho_{\max}$ within one order of magnitude leads to very little change of $(M_1^{\pm\pm}, M_2^{\pm\pm})$ or m_h. Changing $\rho_{\max}$, however, has significant impact on v_R. Generally larger $\rho_{\max}$ leads to smaller v_R, which is the reason why we use a small $\rho_{\max}$ here.

With the above parameter setting, we scan the parameter space and compute the mass spectrum of the doubly charged Higgs bosons when the sample satisfies the global minimum requirements. The result is shown in figure 6, where the yellow, green, and blue regions are the allowed regions by the global minimum requirements for $\rho_2 = 0.1\rho_{\max}$, $0.2\rho_{\max}$, and $0.5\rho_{\max}$ respectively. Note that the constraints presented in figure 6 are only for a very specific parameter setting so they should not be interpreted as universal constraints on the mass spectra. Changing the parameter setting can easily lead to significant changes of the constraints, as illustrated by different values of ρ_2 in figure 6. It is still interesting

JHEP02(2019)154

that there are certain mass ranges for the doubly charged scalars which are forbidden by our analysis and can be used to test the model at the LHC.

6 Conclusion

We have performed a study on the vacuum structure of the left-right symmetric scalar potential. The goal was to investigate whether the usually considered VEV alignment in eq. (2.10) can be obtained from a generic scalar potential as a global minimum. General criteria to identify a charge conserving and parity violating vacuum were derived [see eq. (3.18)], and it was demonstrated that the potential parameters are subject to many constraints in order to achieve this minimum. In general, if we do not put any constraints on the potential parameters, as indicated by figure 3, the probability to end up within the desired VEV alignment is very low, only 0.05%.

We have also analytically studied the minima of the potential in the absence of some terms and obtained sufficient (but not necessary) conditions, given by eqs. (4.23)–(4.26), that enable us to obtain the correct VEV alignment more easily, as shown in figure 4. By requiring that the corresponding minimum is global in this case, we also illustrate the constraints on the potential parameters in figure 5.

Our work suggests that successful generation of the usually considered VEV alignment in standard left-right symmetric theories and keeping the vacuum absolutely stable would produce important constraints on the parameters of the potential. These constraints may have interesting phenomenological consequences such as constraints on the mass spectrum of scalar bosons, or the Higgs self-couplings, which can be used to test the model at the LHC. We have illustrated this with the example of doubly charged scalar masses in the model in figure 6.

The present paper can be a starting point for further, more involved analyses along these lines, such as analyzing loop-corrected effective potentials, investigating the vacuum lifetime of non-global minima, more phenomenological consequences of the global minima, or studies of alternative left-right symmetric models.

Acknowledgments

We thank Werner Porod for clarifying comments. We also thank K.S. Babu, Garv Chauhan and Yongchao Zhang for discussions on related topics. The work of B.D. is supported by the U.S. Department of Energy under Grant No. DE-SC0017987, R.N.M. is supported by the U.S. National Science Foundation under Grant No. PHY1620074, and W.R. is supported by the DFG with grant RO 2516/7-1 in the Heisenberg program.

JHEP02(2019)154

A Deriviation of the seesaw relation between triplet VEVs

In this appendix, we review the derivation of the seesaw relation between the left and right triplet VEVs. To do this, we first compute the six derivatives in eq. (3.5) explicitly:

$$\begin{aligned}0 = \frac{\partial V}{\partial \kappa_1} &= 8\kappa_2^2\kappa_1\lambda_2\cos 2\theta_2 + 2\kappa_1^3\lambda_1 + 2\kappa_2^2\kappa_1\lambda_1 + 4\kappa_2^2\kappa_1\lambda_3 - 2\kappa_1\mu_1^2 \\ &\quad + 2\kappa_2\cos\theta_2\left(3\kappa_1^2\lambda_4 + \kappa_2^2\lambda_4 - 2\mu_2^2 + \alpha_2 v_L^2 + \alpha_2 v_R^2\right) \\ &\quad + 2\beta_2\kappa_1 v_L v_R\cos\theta_L + \beta_1\kappa_2 v_L v_R\cos\left(\theta_2 - \theta_L\right) + \alpha_1\kappa_1 v_L^2 + \alpha_1\kappa_1 v_R^2\,,\end{aligned} \tag{A.1}$$

$$\begin{aligned}0 = \frac{\partial V}{\partial \kappa_2} &= 8\kappa_1^2\kappa_2\lambda_2\cos 2\theta_2 + 2\kappa_2^3\lambda_1 + 2\kappa_1^2\kappa_2\lambda_1 + 4\kappa_1^2\kappa_2\lambda_3 - 2\kappa_2\mu_1^2 \\ &\quad + 2\kappa_1\cos\theta_2\left(\kappa_1^2\lambda_4 + 3\kappa_2^2\lambda_4 - 2\mu_2^2 + \alpha_2 v_L^2 + \alpha_2 v_R^2\right) \\ &\quad + 2\beta_3\kappa_2 v_L v_R\cos\left(2\theta_2 - \theta_L\right) + \beta_1\kappa_1 v_L v_R\cos\left(\theta_2 - \theta_L\right) \\ &\quad + \alpha_1\kappa_2 v_L^2 + \alpha_3\kappa_2 v_L^2 + \alpha_1\kappa_2 v_R^2 + \alpha_3\kappa_2 v_R^2\,,\end{aligned} \tag{A.2}$$

$$\begin{aligned}0 = \frac{\partial V}{\partial v_R} &= \rho_3 v_L^2 v_R + \beta_2\kappa_1^2 v_L\cos\theta_L + \beta_3\kappa_2^2 v_L\cos\left(2\theta_2 - \theta_L\right) + \beta_1\kappa_1\kappa_2 v_L\cos\left(\theta_2 - \theta_L\right) \\ &\quad + 4\alpha_2\kappa_1\kappa_2 v_R\cos\theta_2 + \alpha_1\kappa_1^2 v_R + \alpha_1\kappa_2^2 v_R + \alpha_3\kappa_2^2 v_R - 2\mu_3^2 v_R + 2\rho_1 v_R^3\,,\end{aligned} \tag{A.3}$$

$$\begin{aligned}0 = \frac{\partial V}{\partial v_L} &= \beta_2\kappa_1^2 v_R\cos\theta_L + \beta_3\kappa_2^2 v_R\cos\left(2\theta_2 - \theta_L\right) + \beta_1\kappa_1\kappa_2 v_R\cos\left(\theta_2 - \theta_L\right) + \rho_3 v_L v_R^2 \\ &\quad + 4\alpha_2\kappa_1\kappa_2 v_L\cos\theta_2 + \alpha_1\kappa_1^2 v_L + \alpha_1\kappa_2^2 v_L + \alpha_3\kappa_2^2 v_L - 2\mu_3^2 v_L + 2\rho_1 v_L^3\,,\end{aligned} \tag{A.4}$$

$$\begin{aligned}0 = \frac{\partial V}{\partial \theta_2} &= -8\kappa_2^2\kappa_1^2\lambda_2\sin 2\theta_2 - 2\kappa_1\kappa_2\sin\theta_2\left(\kappa_1^2\lambda_4 + \kappa_2^2\lambda_4 - 2\mu_2^2 + \alpha_2 v_L^2 + \alpha_2 v_R^2\right) \\ &\quad - v_L v_R\kappa_2\left(\beta_1\kappa_1\sin\left(\theta_2 - \theta_L\right) + 2\beta_3\kappa_2\sin\left(2\theta_2 - \theta_L\right)\right),\end{aligned} \tag{A.5}$$

$$0 = \frac{\partial V}{\partial \theta_L} = -\beta_2\kappa_1^2 v_L v_R\sin\theta_L + \beta_1\kappa_2\kappa_1 v_L v_R\sin\left(\theta_2 - \theta_L\right) + \beta_3\kappa_2^2 v_L v_R\sin\left(2\theta_2 - \theta_L\right). \tag{A.6}$$

The first three equations can be regarded as linear equations in terms of μ_1^2, μ_2^2, and μ_3^2, which can be solved without much effort:

$$\begin{aligned}\mu_1^2 &= \frac{\left(\alpha_1\kappa_1^2 - \alpha_1\kappa_2^2 - \alpha_3\kappa_2^2\right)\left(v_L^2 + v_R^2\right)}{2\left(\kappa_1^2 - \kappa_2^2\right)} + \frac{v_L v_R\left(\beta_2\kappa_1^2\cos\theta_L - \beta_3\kappa_2^2\cos\left(2\theta_2 - \theta_L\right)\right)}{\kappa_1^2 - \kappa_2^2} \\ &\quad + 2\kappa_2\kappa_1\lambda_4\cos\theta_2 + \kappa_1^2\lambda_1 + \kappa_2^2\lambda_1\,,\end{aligned} \tag{A.7}$$

$$\begin{aligned}\mu_2^2 &= \kappa_1\kappa_2\sec\theta_2\left(2\lambda_2\cos 2\theta_2 + \lambda_3\right) + \frac{1}{2}\left(\kappa_1^2 + \kappa_2^2\right)\lambda_4 + \left(v_L^2 + v_R^2\right)\left(\frac{\alpha_3\kappa_1\kappa_2\sec\theta_2}{4\left(\kappa_1^2 - \kappa_2^2\right)} + \frac{\alpha_2}{2}\right) \\ &\quad + \frac{\kappa_1\kappa_2 v_L v_R\left[\beta_3\cos\left(2\theta_2 - \theta_L\right) - \beta_2\cos\theta_L\right]\sec\theta_2}{2\left(\kappa_1^2 - \kappa_2^2\right)} + \frac{1}{4}\beta_1 v_L v_R\sec\theta_2\cos\left(\theta_2 - \theta_L\right),\end{aligned} \tag{A.8}$$

JHEP02(2019)154

$$\mu_3^2 = 2\alpha_2\kappa_1\kappa_2\cos\theta_2 + \frac{1}{2}\alpha_3\kappa_2^2 + \frac{1}{2}\alpha_1\left(\kappa_1^2+\kappa_2^2\right) + \frac{1}{2}\rho_3 v_L^2 + \rho_1 v_R^2 + \frac{v_L\left[\beta_2\kappa_1^2\cos\theta_L + \beta_1\kappa_2\kappa_1\cos\left(\theta_2-\theta_L\right) + \beta_3\kappa_2^2\cos\left(2\theta_2-\theta_L\right)\right]}{2v_R}\,. \tag{A.9}$$

Then substituting the solutions of μ_1^2, μ_2^2 , and μ_3^2 into eq. (A.4) gives

$$\left(v_L^2-v_R^2\right)\left[\beta_2\kappa_1^2\cos\theta_L+\cos\left(\theta_2-\theta_L\right)\beta_1\kappa_2\kappa_1+\cos\left(2\theta_2-\theta_L\right)\beta_3\kappa_2^2-\left(2\rho_1-\rho_3\right)v_L v_R\right] = 0\,, \tag{A.10}$$

which for $v_L^2 - v_R^2 \neq 0$ leads to the seesaw relation (3.6).

References

[1] P. Minkowski, *$\mu \to e\gamma$ at a Rate of One Out of 10^9 Muon Decays?*, *Phys. Lett.* **B 67** (1977) 421 [INSPIRE].

[2] R.N. Mohapatra and G. Senjanović, *Neutrino Mass and Spontaneous Parity Nonconservation*, *Phys. Rev. Lett.* **44** (1980) 912 [INSPIRE].

[3] T. Yanagida, *Horizontal gauge symmetry and masses of neutrinos*, *Conf. Proc.* **C 7902131** (1979) 95 [INSPIRE].

[4] M. Gell-Mann, P. Ramond and R. Slansky, *Complex Spinors and Unified Theories*, *Conf. Proc.* **C 790927** (1979) 315 [arXiv:1306.4669] [INSPIRE].

[5] S.L. Glashow, *The Future of Elementary Particle Physics*, *NATO Sci. Ser.* **B 61** (1980) 687 [INSPIRE].

[6] H. Fritzsch and P. Minkowski, *Unified Interactions of Leptons and Hadrons*, *Annals Phys.* **93** (1975) 193 [INSPIRE].

[7] J.C. Pati and A. Salam, *Lepton Number as the Fourth Color*, *Phys. Rev.* **D 10** (1974) 275 [*Erratum ibid.* **D 11** (1975) 703] [INSPIRE].

[8] R.N. Mohapatra and J.C. Pati, *A Natural Left-Right Symmetry*, *Phys. Rev.* **D 11** (1975) 2558 [INSPIRE].

[9] G. Senjanović and R.N. Mohapatra, *Exact Left-Right Symmetry and Spontaneous Violation of Parity*, *Phys. Rev.* **D 12** (1975) 1502 [INSPIRE].

[10] R.N. Mohapatra and R.E. Marshak, *Local $B-L$ Symmetry of Electroweak Interactions, Majorana Neutrinos and Neutron Oscillations*, *Phys. Rev. Lett.* **44** (1980) 1316 [*Erratum ibid.* **44** (1980) 1643] [INSPIRE].

[11] G.C. Branco and L. Lavoura, *Natural CP Breaking in Left-right Symmetric Theories*, *Phys. Lett.* **B 165** (1985) 327 [INSPIRE].

[12] J. Basecq, J. Liu, J. Milutinovic and L. Wolfenstein, *Spontaneous CP Violation in $\mathrm{SU}(2)_L \times \mathrm{SU}(2)_R \times \mathrm{U}(1)_{B-L}$ Models*, *Nucl. Phys.* **B 272** (1986) 145 [INSPIRE].

[13] J.F. Gunion, J. Grifols, A. Mendez, B. Kayser and F.I. Olness, *Higgs Bosons in Left-Right Symmetric Models*, *Phys. Rev.* **D 40** (1989) 1546 [INSPIRE].

JHEP02(2019)154

[14] N.G. Deshpande, J.F. Gunion, B. Kayser and F.I. Olness, *Left-right symmetric electroweak models with triplet Higgs*, *Phys. Rev.* **D 44** (1991) 837 [INSPIRE].

[15] P. Duka, J. Gluza and M. Zralek, *Quantization and renormalization of the manifest left-right symmetric model of electroweak interactions*, *Annals Phys.* **280** (2000) 336 [hep-ph/9910279] [INSPIRE].

[16] G. Barenboim, M. Gorbahn, U. Nierste and M. Raidal, *Higgs Sector of the Minimal Left-Right Symmetric Model*, *Phys. Rev.* **D 65** (2002) 095003 [hep-ph/0107121] [INSPIRE].

[17] K. Kiers, M. Assis and A.A. Petrov, *Higgs sector of the left-right model with explicit CP-violation*, *Phys. Rev.* **D 71** (2005) 115015 [hep-ph/0503115] [INSPIRE].

[18] J. Chakrabortty, P. Konar and T. Mondal, *Constraining a class of $B-L$ extended models from vacuum stability and perturbativity*, *Phys. Rev.* **D 89** (2014) 056014 [arXiv:1308.1291] [INSPIRE].

[19] J. Chakrabortty, P. Konar and T. Mondal, *Copositive Criteria and Boundedness of the Scalar Potential*, *Phys. Rev.* **D 89** (2014) 095008 [arXiv:1311.5666] [INSPIRE].

[20] R.N. Mohapatra and Y. Zhang, *TeV Scale Universal Seesaw, Vacuum Stability and Heavy Higgs*, *JHEP* **06** (2014) 072 [arXiv:1401.6701] [INSPIRE].

[21] T. Mondal, U.K. Dey and P. Konar, *Implications of unitarity and charge breaking minima in a left-right symmetric model*, *Phys. Rev.* **D 92** (2015) 096005 [arXiv:1508.04960] [INSPIRE].

[22] P.S.B. Dev, R.N. Mohapatra and Y. Zhang, *Probing the Higgs Sector of the Minimal Left-Right Symmetric Model at Future Hadron Colliders*, *JHEP* **05** (2016) 174 [arXiv:1602.05947] [INSPIRE].

[23] A. Maiezza, M. Nemevšek and F. Nesti, *Perturbativity and mass scales in the minimal left-right symmetric model*, *Phys. Rev.* **D 94** (2016) 035008 [arXiv:1603.00360] [INSPIRE].

[24] J. Chakrabortty, J. Gluza, T. Jelinski and T. Srivastava, *Theoretical constraints on masses of heavy particles in Left-Right Symmetric Models*, *Phys. Lett.* **B 759** (2016) 361 [arXiv:1604.06987] [INSPIRE].

[25] A. Maiezza, G. Senjanović and J.C. Vasquez, *Higgs sector of the minimal left-right symmetric theory*, *Phys. Rev.* **D 95** (2017) 095004 [arXiv:1612.09146] [INSPIRE].

[26] B. Brahmachari, M.K. Samal and U. Sarkar, *Potential minimization in left-right symmetric models*, hep-ph/9402323 [INSPIRE].

[27] J. Choi and R.R. Volkas, *The Effective potential at finite temperature in the left-right symmetric model*, *Phys. Rev.* **D 48** (1993) 1258 [hep-ph/9210223] [INSPIRE].

[28] K.S. Babu and A. Patra, *Higgs Boson Spectra in Supersymmetric Left-Right Models*, *Phys. Rev.* **D 93** (2016) 055030 [arXiv:1412.8714] [INSPIRE].

[29] L. Basso, B. Fuks, M.E. Krauss and W. Porod, *Doubly-charged Higgs and vacuum stability in left-right supersymmetry*, *JHEP* **07** (2015) 147 [arXiv:1503.08211] [INSPIRE].

[30] X.-J. Xu, *Tree-level vacuum stability of two-Higgs-doublet models and new constraints on the scalar potential*, *Phys. Rev.* **D 95** (2017) 115019 [arXiv:1705.08965] [INSPIRE].

[31] X.-J. Xu, *Minima of the scalar potential in the type-II seesaw model: From local to global*, *Phys. Rev.* **D 94** (2016) 115025 [arXiv:1612.04950] [INSPIRE].

[32] N. Chen, C. Du, Y. Wu and X.-J. Xu, *Further study of the global minimum constraint on the two-Higgs-doublet models: LHC searches for heavy Higgs bosons*, *Phys. Rev.* **D 99** (2019) 035011 [arXiv:1810.04689] [INSPIRE].

JHEP02(2019)154

[33] Y.B. Zeldovich, I.Y. Kobzarev and L.B. Okun, *Cosmological Consequences of the Spontaneous Breakdown of Discrete Symmetry*, *Zh. Eksp. Teor. Fiz.* **67** (1974) 3 [*Sov. Phys. JETP* **40** (1974) 1] [INSPIRE].

[34] S.E. Larsson, S. Sarkar and P.L. White, *Evading the cosmological domain wall problem*, *Phys. Rev.* **D 55** (1997) 5129 [hep-ph/9608319] [INSPIRE].

[35] J.E. Camargo-Molina, B. O'Leary, W. Porod and F. Staub, *Vevacious: A Tool For Finding The Global Minima Of One-Loop Effective Potentials With Many Scalars*, *Eur. Phys. J.* **C 73** (2013) 2588 [arXiv:1307.1477] [INSPIRE].

[36] https://github.com/xunjiexu/LR_Vmin.

[37] G. Chauhan, P.S.B. Dev, R.N. Mohapatra and Y. Zhang, *Perturbativity constraints on $U(1)_{B-L}$ and left-right models and implications for heavy gauge boson searches*, *JHEP* **01** (2019) 208 [arXiv:1811.08789] [INSPIRE].

[38] V. Tello, M. Nemevšek, F. Nesti, G. Senjanović and F. Vissani, *Left-Right Symmetry: from LHC to Neutrinoless Double Beta Decay*, *Phys. Rev. Lett.* **106** (2011) 151801 [arXiv:1011.3522] [INSPIRE].

[39] M. Nemevšek, F. Nesti, G. Senjanović and Y. Zhang, *First Limits on Left-Right Symmetry Scale from LHC Data*, *Phys. Rev.* **D 83** (2011) 115014 [arXiv:1103.1627] [INSPIRE].

[40] S.P. Das, F.F. Deppisch, O. Kittel and J.W.F. Valle, *Heavy Neutrinos and Lepton Flavour Violation in Left-Right Symmetric Models at the LHC*, *Phys. Rev.* **D 86** (2012) 055006 [arXiv:1206.0256] [INSPIRE].

[41] J. Barry and W. Rodejohann, *Lepton number and flavour violation in TeV-scale left-right symmetric theories with large left-right mixing*, *JHEP* **09** (2013) 153 [arXiv:1303.6324] [INSPIRE].

[42] P.S.B. Dev, S. Goswami, M. Mitra and W. Rodejohann, *Constraining neutrino mass from neutrinoless double beta decay*, *Phys. Rev.* **D 88** (2013) 091301 [arXiv:1305.0056] [INSPIRE].

[43] C.-Y. Chen, P.S.B. Dev and R.N. Mohapatra, *Probing Heavy-Light Neutrino Mixing in Left-Right Seesaw Models at the LHC*, *Phys. Rev.* **D 88** (2013) 033014 [arXiv:1306.2342] [INSPIRE].

[44] O. Castillo-Felisola, C.O. Dib, J.C. Helo, S.G. Kovalenko and S.E. Ortiz, *Left-Right Symmetric Models at the High-Intensity Frontier*, *Phys. Rev.* **D 92** (2015) 013001 [arXiv:1504.02489] [INSPIRE].

[45] P.S.B. Dev, D. Kim and R.N. Mohapatra, *Disambiguating Seesaw Models using Invariant Mass Variables at Hadron Colliders*, *JHEP* **01** (2016) 118 [arXiv:1510.04328] [INSPIRE].

[46] G. Bambhaniya, P.S.B. Dev, S. Goswami and M. Mitra, *The scalar triplet contribution to lepton flavour violation and neutrinoless double beta decay in Left-Right Symmetric Model*, *JHEP* **04** (2016) 046 [arXiv:1512.00440] [INSPIRE].

[47] M. Lindner, F.S. Queiroz and W. Rodejohann, *Dilepton bounds on left-right symmetry at the LHC run II and neutrinoless double beta decay*, *Phys. Lett.* **B 762** (2016) 190 [arXiv:1604.07419] [INSPIRE].

[48] M. Lindner, F.S. Queiroz, W. Rodejohann and C.E. Yaguna, *Left-Right Symmetry and Lepton Number Violation at the Large Hadron Electron Collider*, *JHEP* **06** (2016) 140 [arXiv:1604.08596] [INSPIRE].

JHEP02(2019)154

[49] C. Bonilla, M.E. Krauss, T. Opferkuch and W. Porod, *Perspectives for Detecting Lepton Flavour Violation in Left-Right Symmetric Models*, *JHEP* **03** (2017) 027 [arXiv:1611.07025] [INSPIRE].

[50] M. Nemevšek, F. Nesti and J.C. Vasquez, *Majorana Higgses at colliders*, *JHEP* **04** (2017) 114 [arXiv:1612.06840] [INSPIRE].

[51] P. Fileviez Perez and C. Murgui, *Lepton Flavour Violation in Left-Right Theory*, *Phys. Rev.* **D 95** (2017) 075010 [arXiv:1701.06801] [INSPIRE].

[52] P.S.B. Dev, R.N. Mohapatra and Y. Zhang, *Long Lived Light Scalars as Probe of Low Scale Seesaw Models*, *Nucl. Phys.* **B 923** (2017) 179 [arXiv:1703.02471] [INSPIRE].

[53] S. Mandal, M. Mitra and N. Sinha, *Constraining the right-handed gauge boson mass from lepton number violating meson decays in a low scale left-right model*, *Phys. Rev.* **D 96** (2017) 035023 [arXiv:1705.01932] [INSPIRE].

[54] M. Nemevšek, F. Nesti and G. Popara, *Keung-Senjanović process at the LHC: From lepton number violation to displaced vertices to invisible decays*, *Phys. Rev.* **D 97** (2018) 115018 [arXiv:1801.05813] [INSPIRE].

[55] J. Barry, L. Dorame and W. Rodejohann, *Linear collider test of a neutrinoless double beta decay mechanism in left-right symmetric theories*, *Eur. Phys. J.* **C 72** (2012) 2023 [arXiv:1203.3365] [INSPIRE].

[56] P.S.B. Dev and Y. Zhang, *Displaced vertex signatures of doubly charged scalars in the type-II seesaw and its left-right extensions*, *JHEP* **10** (2018) 199 [arXiv:1808.00943] [INSPIRE].

[57] G. Senjanović, *Spontaneous Breakdown of Parity in a Class of Gauge Theories*, *Nucl. Phys.* **B 153** (1979) 334 [INSPIRE].

[58] D. Chang, R.N. Mohapatra and M.K. Parida, *A New Approach to Left-Right Symmetry Breaking in Unified Gauge Theories*, *Phys. Rev.* **D 30** (1984) 1052 [INSPIRE].

[59] E.K. Akhmedov, M. Lindner, E. Schnapka and J.W.F. Valle, *Dynamical left-right symmetry breaking*, *Phys. Rev.* **D 53** (1996) 2752 [hep-ph/9509255] [INSPIRE].

[60] B. Brahmachari, E. Ma and U. Sarkar, *Truly minimal left right model of quark and lepton masses*, *Phys. Rev. Lett.* **91** (2003) 011801 [hep-ph/0301041] [INSPIRE].

[61] M. Malinsky, J.C. Romao and J.W.F. Valle, *Novel supersymmetric* SO(10) *seesaw mechanism*, *Phys. Rev. Lett.* **95** (2005) 161801 [hep-ph/0506296] [INSPIRE].

[62] P.S.B. Dev and R.N. Mohapatra, *TeV Scale Inverse Seesaw in* SO(10) *and Leptonic Non-Unitarity Effects*, *Phys. Rev.* **D 81** (2010) 013001 [arXiv:0910.3924] [INSPIRE].

[63] M. Holthausen, M. Lindner and M.A. Schmidt, *Radiative Symmetry Breaking of the Minimal Left-Right Symmetric Model*, *Phys. Rev.* **D 82** (2010) 055002 [arXiv:0911.0710] [INSPIRE].

[64] J. Chakrabortty, *Type I and new seesaw in left-right symmetric theories*, *Phys. Lett.* **B 690** (2010) 382 [arXiv:1005.1377] [INSPIRE].

[65] D. Borah, S. Patra and U. Sarkar, *TeV scale Left Right Symmetry with spontaneous D-parity breaking*, *Phys. Rev.* **D 83** (2011) 035007 [arXiv:1006.2245] [INSPIRE].

[66] J. Heeck and S. Patra, *Minimal Left-Right Symmetric Dark Matter*, *Phys. Rev. Lett.* **115** (2015) 121804 [arXiv:1507.01584] [INSPIRE].

[67] W. Rodejohann and X.-J. Xu, *A left-right symmetric flavor symmetry model*, *Eur. Phys. J.* **C 76** (2016) 138 [arXiv:1509.03265] [INSPIRE].

JHEP02(2019)154

[68] V. Brdar and A.Y. Smirnov, *Low Scale Left-Right Symmetry and Naturally Small Neutrino Mass*, *JHEP* **02** (2019) 045 [arXiv:1809.09115] [INSPIRE].

[69] C. Majumdar, S. Patra, S. Senapati and U.A. Yajnik, *Neutrinoless double beta decay in a minimal left-right symmetric model with gauge coupling unification*, arXiv:1809.10577 [INSPIRE].

[70] R.N. Mohapatra and G. Senjanović, *Neutrino Masses and Mixings in Gauge Models with Spontaneous Parity Violation*, *Phys. Rev.* **D 23** (1981) 165 [INSPIRE].

[71] J. Nocedal, *Numerical optimization*, Springer, New York U.S.A. (2006).

JHEP02(2019)154